NASA CONTRACTOR REPORT

NASA CR-2126

NASA CR-2126

NOISE FROM INTERACTION OF FLOW WITH RIGID SURFACES: A REVIEW OF CURRENT STATUS OF PREDICTION TECHNIQUES

by Richard E. Hayden

Prepared by
BOLT BERANEK AND NEWMAN, INC.
Cambridge, Mass. 02138
for Langley Research Center

NATIONAL AERONAUTICS AND SPACE ADMINISTRATION • WASHINGTON, D. C. • OCTOBER 1972

1. Report No.	2. Government Accession No.	3. Recipient's Catalog No.
NASA CR-2126		

4. Title and Subtitle	5. Report Date
NOISE FROM INTERACTION OF FLOW WITH RIGID SURFACES: A REVIEW OF CURRENT STATUS OF PREDICTION TECHNIQUES	October 1972
	6. Performing Organization Code

7. Author(s)	8. Performing Organization Report No.
BY RICHARD E. HAYDEN	2276
	10. Work Unit No.

9. Performing Organization Name and Address	11. Contract or Grant No.
Bolt Beranek and Newman, Inc. 50 Moulton Street Cambridge, MA 02138	NAS1-9559-14
	13. Type of Report and Period Covered
12. Sponsoring Agency Name and Address	Contractor Report
National Aeronautics and Space Administration Washington, D.C. 20546	14. Sponsoring Agency Code

15. Supplementary Notes

16. Abstract

A brief review of some fundamental aspects of sound arising from turbulent boundary layers, noise due to flow past a single discontinuity (trailing edge), noise from airfoils operating in turbulent flow, and noise due to rigid flow discontinuities (spoilers) immersed in rigid ducts is presented. Emphasis is on dipole-like sound fields associated with turbulent flow past a trailing edge, rigid bodies in turbulence and in-duct spoilers. Representative available data are reviewed and evaluated in terms of theoretical considerations and, where possible, empirical prediction techniques are given in terms of convenient aerodynamic and geometric parameters. Limitations on current knowledge are discussed.

17. Key Words (Suggested by Author(s))	18. Distribution Statement
Noise Aircraft Noise Airflow Interaction Noise	Unclassified-Unlimited

19. Security Classif. (of this report)	20. Security Classif. (of this page)	21. No. of Pages	22. Price*
Unclassified	Unclassified	64	$3.00

*For sale by the National Technical Information Service, Springfield, Virginia 22151

FOREWORD

The work presented in this report was performed by Bolt Beranek and Newman Inc., Cambridge, Massachusetts under NASA Contract No. NAS1-9559-14 and administered by the Acoustics Branch, Loads Division, NASA Langley Research Center, Hampton, Virginia. The report covers material available in the public domain prior to October 1971. In some of the areas covered, there is a considerable volume of related experimental data which is in essential agreement. In such cases, only a representative sample was cited. Any omission of reference to significant related works is not intended as an implicit evaluation of the work.

The author gratefully acknowledges helpful discussions with and contributions of his colleagues Drs. R. C. Chanaud, K. L. Chandiramani and H. H. Heller. The cooperation of Mr. H. H. Hubbard of NASA Langley Research Center in providing current data for evaluation is gratefully acknowledged.

This report has been assigned Bolt Beranek and Newman Inc. Report No. 2276.

TABLE OF CONTENTS

	page
FOREWORD	iii
LIST OF FIGURES AND TABLES	vi
LIST OF SYMBOLS	ix
SUMMARY	1
INTRODUCTION	1
Statement of the General Problem	1
Scope of this Report	5
SOUND RADIATION BY FLOW PAST A SINGLE DISCONTINUITY: TRAILING EDGE NOISE	6
Theoretical Considerations	6
Summary of Experimental Observations: Flow on One Side of Surface	9
Flow on Both Sides of an Edge	19
Empirical Formulations	20
Illustrative Calculations	24
SOUND RADIATION BY RIGID BODIES IN DISTURBED INFLOWS	31
General Discussion of Source Characteristics	31
Effect of Deviation from Point Dipole Regime	39
Empirical Formulations	39
SOUND RADIATION FROM FLOW SPOILERS IN A CONFINED ENVIRONMENT	41
Theoretical Treatment	41
Empirical Formulations	44
CLOSING	51
REFERENCES	52

LIST OF FIGURES AND TABLES

Figure		page
1	Block Diagram of Typical Flow Noise Problem	2
2	Schematic of Fluid Inputs and Acoustic Sources	3
3	Sound Source Due to Turbulent Flow Past a Trailing Edge	7
4	Coordinate System and Terminology	10
5	Three-Dimensional Wall Jet Characteristics	11
6	Normalized 1/3 Octave Band Spectra of Trailing Edge Noise	12
7	Comparison of Trailing Edge Noise Data	13
8	Directivity of Trailing Edge Noise Source When KL > 1	15
9	Observed Reduction of "Edge Sound Power" Due to Edge Thickness [Reference 9]	17
10	Trailing Edge Noise From a Three-Dimensional Nozzle/Plate System	18
11	Normalized Spectrum of Wake-Generated Noise; Semi-Infinite Flat Plate	21
12	Calculation of Trailing Edge Noise From a Thin Flat Plate Moving in Still Air at 300 fps	26
13	Comparison of Predicted Airfoil Noise Spectrum with Measurement	29
14	Coordinate System for Computing Point Dipole Sound Field	34
15	Sound Pressure Level Directivity for Free-Field Point Dipole	35
16	Lift Response of Finite Span Airfoils in 2- and 3-Dimensional Inflows	40

LIST OF FIGURES AND TABLES (Cont.)

Figures page

17 Spoiler-in-Duct Geometry 42

18 Change of Sound Power Output for Spoiler Source In-Duct and Free-Field 43

19 Empirical Curve for Prediction of Spoiler Noise 46

20 Nomogram for Predicting Spoiler Noise from Pressure Drop and Duct Diameter 49

Table I 50

LIST OF SYMBOLS

a	characteristic radius of a source
A	area
b	span of an airfoil or edge
c	sound speed
C	chord length, or lift coefficient (C_L)
d	characteristic cross-sectional dimension of flow spoiler
D	duct diameter
f	frequency (hertz)
h or H	nozzle (or slot) height
i	$\equiv \sqrt{-1}$
I	acoustic intensity
k	acoustic wavenumber or normalized turbulence wavenumber; also normalization factor for spoiler noise
ℓ	correlation dimension of turbulent eddy or wall pressure disturbance
L	plate length
L	integral correlation length
m	spanwise turbulent wavenumber
p	fluctuating pressure
PWL	sound power level (in dB re 10^{-12} watts)
q	dynamic pressure (= $1/2\ \rho U^2$)
r	generalized radial distance
R	specific (or fixed) radial distance
S	surface area

LIST OF SYMBOLS (Cont.)

SPL	sound pressure level (dB re 0.0002 μbar)
t	time
T	thickness of an edge
u	longitudinal (streamwise) velocity fluctuation
U	mean velocity
v	transverse velocity fluctuation
w	velocity fluctuation normal to mean flow and surface (i.e., upwash velocity); also spanwise correlation length
W	absolute value of upwash velocity; also width of edge
x	streamwise coordinate
y	spanwise coordinate
z	normal (to flow and surface) coordinate

Greek symbols:

α	angle of attack
δ	characteristic dimension of a flow disturbance (such as boundary layer thickness)
θ	spherical angle
λ	acoustic wavelength
ν	kinematic viscosity of fluid
Π	sound power
ρ	fluid density
Φ	spectral density
ψ	angle in plane normal to $\theta = 0$ axis

LIST OF SYMBOLS (Cont.)

ψ	Sear's function
ω	circular (radian) frequency (in radians/sec.)

Subscripts:

c	characteristic or correlation length
e	pertaining to a turbulent eddy
j	jet
L	at full length of a body
m	mean value or maximum local velocity
N	normalized
o	pertaining to ambient or initial condition
OA	overall
r	in the radial direction
s	pertaining to source
t	total
w	at a wall or at surface also, pertaining to wake
x	in the x-direction
y	in the y-direction

Superscripts:

$(\dot{})$ or $(\,)'$	fluctuating component
$(\overline{\qquad\qquad})$	mean of quantity in parentheses

NOISE FROM INTERACTION OF FLOW WITH RIGID SURFACES: A REVIEW OF CURRENT STATUS OF PREDICTION TECHNIQUES

by Richard E. Hayden
Bolt Beranek and Newman Inc.

SUMMARY

The purpose of this report is to provide background information on existing techniques which may be used to predict sound radiation by several classes of flow interactions with rigid surfaces. Those theoretical approaches which have received reasonable experimental confirmation are amenable to the development of empirical prediction techniques which may be employed by proper matching of prediction scheme with aerodynamic, acoustic, and geometric parameters. Such a task is not trivial and requires an awareness of restrictions on current knowledge.

This report discusses some fundamental aspects of sound arising from turbulent boundary layers, noise due to flow past a single discontinuity (trailing edge), noise from airfoils operating in turbulent flow, and noise due to rigid flow discontinuities (spoilers) immersed in rigid ducts. Representative available data are reviewed and evaluated in terms of theoretical considerations and, where possible, empirical prediction techniques are given in terms of convenient aerodynamic and geometric parameters.

INTRODUCTION

Statement of the General Problem

The introduction of surfaces into fluid flows results in conversion of some of the energy in the flow into sound. For the cases of concern here, the fluid will be assumed viscous and obviously must be compressible for sound to result. The viscosity condition implies that viscous shear will, under many conditions, produce turbulence in the flow, either in the "free" part of the flow, or near the fluid/surface boundaries. Thus, we might restate the problem: *the introduction of surfaces into fluid flows results in the conversion of incompressible pressure (or velocity) fluctuations which are travelling subsonically into compressible pressure fluctuations which then propagate away from the surface at the sound speed of the medium.*

Prediction of noise production by flows interacting with rigid surfaces is generically similar to predicting the output of any dynamic system due to some arbitrary (but known) input. Specifically, to predict accurately the output of such a system, one must have accurate knowledge of the input and the "transfer function" (Fig. 1).

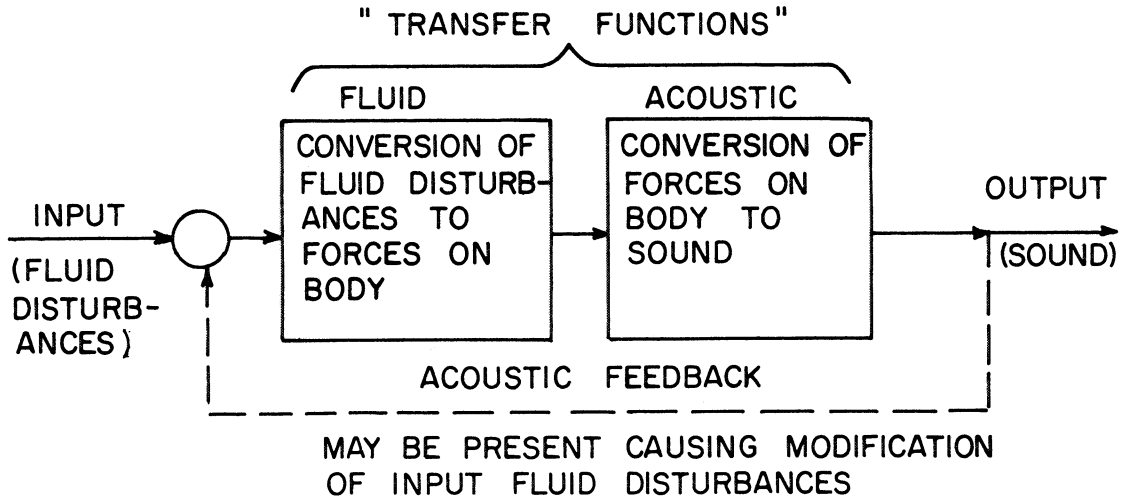

FIG. 1. BLOCK DIAGRAM OF TYPICAL FLOW NOISE PROBLEM

The basic inputs of interest here are fluid disturbances such as free turbulence, boundary layer turbulence, and shed vorticity from a body. Two types of "transfer functions" are typically involved; one being the conversion of the fluid disturbances into pressures or forces on the body (and thus on the surrounding medium) and the other being the conversion of these pressures or forces into sound. Under some conditions, the "output" of this process - acoustic pressure and velocity fluctuations - may influence the input fluid disturbances, thus being analogous to a feedback loop. Figure 2 depicts schematically a typical problem wherein a rigid body is acted upon by some arbitrary flow field to produce sound, and the qualitative manner in which the various types input disturbances are converted to acoustically significant quantities. Sources of fluctuating forces on a fluid medium are characterized as acoustic dipoles, or dipole-like sources. As indicated by the chart in Fig. 2, the nature of the source model depends upon the characteristic frequency of the sound-producing flow disturbance and the characteristic dimensions of the body. Since the parameters frequency, length, scale, and convection (or propagation) speed of both the flow disturbances and the resulting sound are simply related, one may easily and conveniently

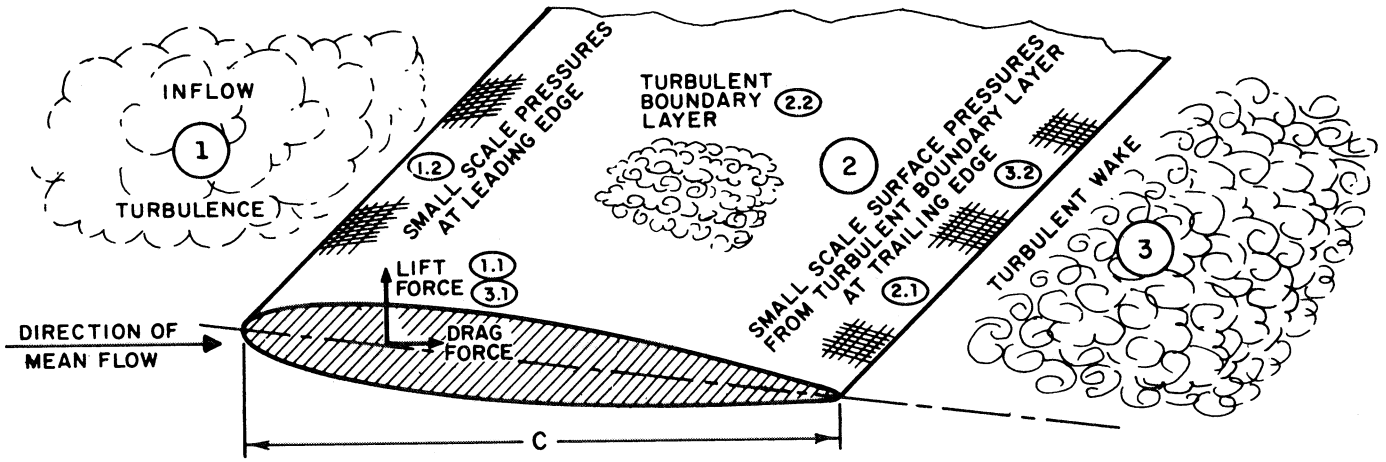

FLUID SOURCE	MAJOR ACOUSTIC SIGNIFICANCE	ACOUSTIC SOURCE MODEL; REGIME
(1) INFLOW TURBULENCE	(1.1) LIFT AND DRAG FLUCTUATIONS OF WHOLE SURFACE	(1.1) POINT DIPOLE; $kC << 1$
	(1.2) SMALL SCALE PRESSURE FLUCTUATIONS AT LEADING EDGE	(1.2) EDGE DIPOLE; $kC >> 1$
(2) TURBULENT BOUNDARY LAYER	(2.1) SMALL SCALE PRESSURE FLUCTUATIONS AT TRAILING EDGE	(2.1) EDGE DIPOLE; $kC >> 1$
	(2.2) ACOUSTICALLY "FAST" PRESSURES THAT RADIATE DIRECTLY	(2.2) "LOW WAVENUMBER" MODEL; $k_c \leq k_a$
(3) TURBULENT WAKE	(3.1) LIFT AND DRAG FLUCTUATIONS ON WHOLE SURFACE	(3.1) POINT DIPOLE; $kC << 1$
	(3.2) SMALL SCALE PRESSURE FLUCTUATIONS AT TRAILING EDGE	(3.2) EDGE DIPOLE; $kC >> 1$

FIG. 2. SCHEMATIC OF FLUID INPUTS AND ACOUSTIC SOURCES

identify and define several different acoustic regimes in which different source models apply. These are*:

(1) *"Point" Source.* The body behaves like a point dipole source when the wavelength λ of the sound produced by the interaction of the flow with the body is large with respect to characteristic dimensions of the body (such as chord length C in Fig. 2). Under these conditions, all parts of the surface are essentially in phase with respect to the fluctuating forces being exerted on the surrounding medium. The point source criterion may be expressed in terms of the acoustic wavenumber k ($= \omega/c_0 = 2\pi/\lambda$) and the source dimension C; the source may be considered to be a point source when $kC << 1$.

(2) *"Half-Baffled" Source - source at edge of a semi-infinite surface (such as "edge dipole").* In many cases, surfaces supporting flow are so much larger than the characteristic scale of the flow disturbances that the net fluctuating force on the surface tends toward zero; i.e., pressures on the surface tend to cancel due to phase and polarity differences. However, potent sound sources are known to exist at the edges where, along the span of the edge, there is incomplete cancellation and each locally coherent pressure patch may independently impart acoustically significant momentum fluctuations to the medium.

When the wavelength of the sound produced by such small scale fluid disturbances interacting with the medium at an edge is small with respect to the dimensions of the surface ($kC \gtrsim 1$), then modified dipole-like sources exist at the edge. The presence of the surface changes the spatial characteristics of the resultant sound field, which qualitatively has the appearance of a half-baffled dipole.

(3) *"Fully-Baffled" Source - direct radiation from the turbulent boundary layer.* On a surface very large in terms of acoustic wavelengths, sound may be radiated directly from the surface layer due to those flow disturbances whose convection (or phase) velocities are greater than the local sound speed of the fluid medium. These "acoustically fast" pressures have wavenumbers (ω/U_c) less than or equal to the critical acoustic

---

*Some of the terms chosen here to identify the various source categories are quite arbitrary and not necessarily universally accepted. In fact, there is currently considerable disagreement over the very nature of some of the sources associated with flow interactions with surfaces.

wavenumber (ω/c_o) where ω is the circular frequency, U_c and c_o are respectively the convection velocity and sound speed.

Scope of This Report

The remainder of this report presents fundamentals and empirical formulations for predicting noise from (1) turbulent boundary layer or turbulent wall jet flow past a trailing edge, (2) airfoils or other rigid surfaces operating in free turbulence, and (3) flow spoilers located in rigid ducts.

The subject of "direct" radiation from turbulent boundary layers will not be treated further here since, despite considerable theoretical activity over the past twenty years, no experimental data exists which can be interpreted as being sufficiently free from extraneous acoustic pressures. Thus, for lack of data, quantitative estimates of the contribution of direct acoustic radiation from a boundary layer cannot be made with a reasonable degree of confidence. Restrictions on applicability of prediction methods for the other sources are discussed in the ensuing text.

SOUND RADIATION BY FLOW PAST A SINGLE DISCONTINUITY: TRAILING EDGE NOISE

The case treated here is the one in which a rigid surface supports a turbulent flow - such as a turbulent boundary layer or a turbulent wall jet - and the leading edge is a large distance from the trailing edge in acoustic wavelengths. In such cases, the pressure fluctuations on the surface tend to cancel except at the trailing edge.

Theoretical Considerations

The convection of turbulent boundary layer or wall jet pressure fluctuations past a trailing edge results in the imparting of momentum fluctuations to the fluid medium at the edge. The edge may in this way be regarded as a pressure release point where the impedance to the hydrodynamic pressure fluctuations in the plane of the surface abruptly changes from infinite to finite (tending toward ρc_o, the characteristic impedance of the medium, as a lower bound). Sources of momentum fluctuations may be appropriately modeled as simple dipole sound sources. Before considering the general distributed source, one might first consider a model for a single eddy encountering the trailing edge of a rigid surface (Fig. 3). If the source of the fluctuating force is regarded as a sphere of radius "a" exerting a force on the medium along a preferred axis, then the source may be approximated by a point dipole model [References 1 and 2] whose sound power may be written

$$\Pi_D(\omega) = \frac{\omega^2 F^2}{12\pi\rho c_o^3} \qquad \text{when } ka << 1 \tag{1}$$

where ω is the characteristic frequency of the force F, ρ is the density of the medium, c_o is the isentropic sound speed, and k is the acoustic wavenumber equal to ω/c_o. Of course, replacing the fluid mechanical source with an oscillating sphere does not accurately represent the physical phenomena but does allow one to visualize qualitative features of this source.

In the edge noise model [References 3,4,5] F is assumed to be proportional to the free-stream dynamic pressure times a correlation area A_c ($F \propto 1/2\rho U^2 A_c$), where A_c is defined as the

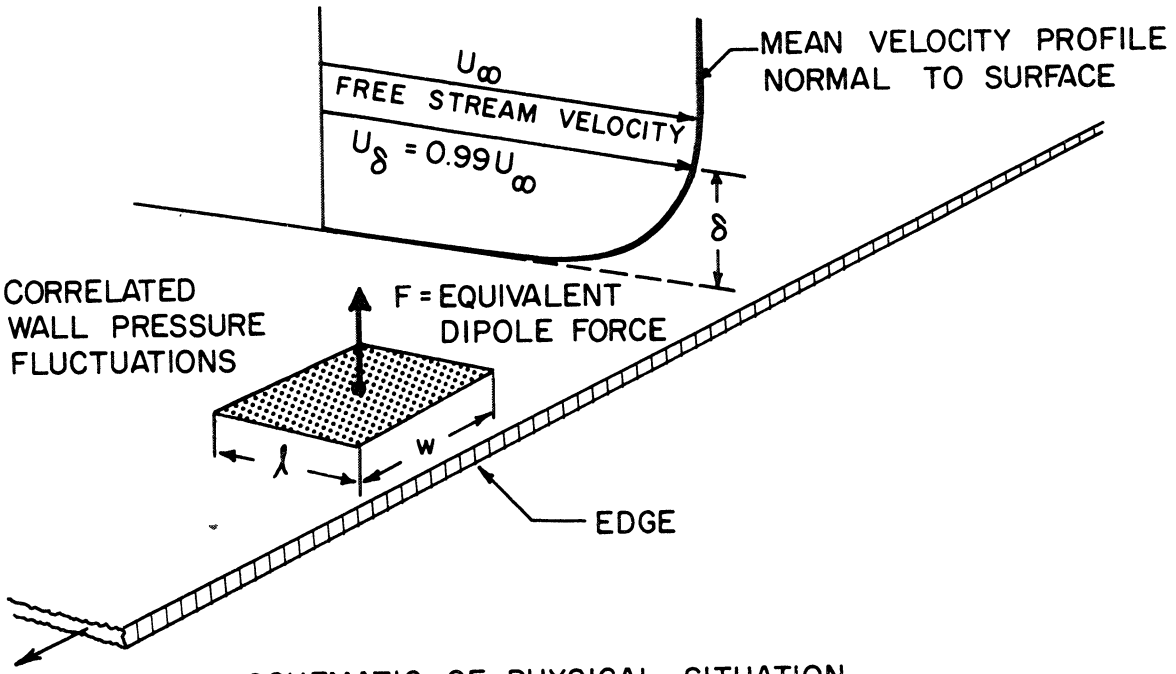

a. SCHEMATIC OF PHYSICAL SITUATION

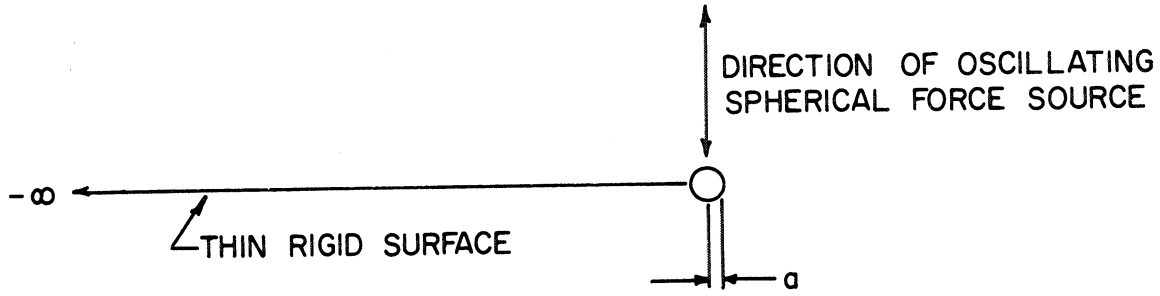

b. "EQUIVALENT" SPHERICAL DIPOLE SOUND SOURCE

FIG. 3. SOUND SOURCE DUE TO TURBULENT FLOW PAST A TRAILING EDGE

product of a longitudinal (streamwise) correlation length ℓ and a spanwise correlation length w. The characteristic frequency of the force (i.e., pressure fluctuations) is usually found to be proportional to U/ℓ (i.e., $f\ell/U$ = constant).

Thus, the sound power from a single eddy encountering the edge is

$$\Pi_D \propto \frac{1}{12\pi\rho c_o^3} \cdot (2\pi U_m/\ell)^2 \quad (1/2\rho U_m^2 \ell w)^2$$

$$= \frac{\pi\, U_m^6 \rho w^2}{12\, c_o^3} \quad . \tag{2}$$

This approach may be extended to develop a model for an edge immersed in a large number of small scale pressure fluctuations. If, over the edge span W, there are n uncorrelated individual sources, n = W/w then the total power from the edge is

$$\Pi_{total} = \frac{W}{w}\,\Pi_D; \quad \Pi_{total} \propto \frac{\pi\rho U_m^6 wW}{12c_o^3} \quad . \tag{3}$$

One feature of this result is the U^6 dependence which was first derived by Curle [Reference 6] for small bodies undergoing fluctuating aerodynamic forces. Since, over a large Mach number or Reynolds number range, turbulence intensities and length scales may vary somewhat with mean velocity, there is no reason to expect *a priori* the U_m^6 law to be obeyed rigorously in all experimental situations.

Since it has been presumed that the fluctuating wall pressure is responsible for the "strength" of the sound source, then it follows that the proportionality constant relating the two sides of Eq. (3) would be on the order of $[p_w/q_m]^2$ - the ratio of fluctuating surface pressure to free-stream dynamic pressure. This ratio is known to vary substantially between various classes of viscous flow fields - usually between the orders of 10^{-1} and 10^{-4} for turbulent boundary layers and turbulent wall jets. However, the current state of knowledge of edge noise does not include adequate documentation of the variation in trailing edge noise over a wide range $[p_w/q_m]$ levels.

The relationship between the two sides of Eq. (3) has been examined experimentally by Hayden and Chanaud using a plane turbulent wall jet flowing over a rigid flat plate (Fig. 4). Wall jet flow fields have, in general, three distinct flow regimes: (1) the "potential core" regime where the wall shear layer beneath the laminar core behaves very much like a turbulent boundary layer; (2) the two-dimensional or "characteristic decay" region where the free shear layer has merged with the wall shear layer and the flow is in a fully-developed turbulent state; (3) the "radial decay" region where the side shear layers have merged and the flow field is fully three-dimensional (see Fig. 5). The measurements by Hayden and Chanaud, made in a large anechoic room, determined the parametric dependence of the trailing edge sound, its directivity, and its nondimensional energy spectrum.

Summary of Experimental Observations:

Flow on One Side of Surface

Dependence on Mean Flow Parameters. In each of the three wall jet flow regimes described above, the overall sound power was found [References 3 and 4] to vary as $(U_m^6 \cdot \delta \cdot W_{1/2})$, as predicted by the source model in Eq. 3. (where $\delta/w = $ constant). In the experimental arrangement used by Hayden and Chanaud, the characteristic wetted span was taken to be $2W_{1/2}$; in two-dimensional flow situations, the characteristic wetted span would be taken to be the entire trailing edge span. The spectra in each flow regime were found to obey a Strouhal number distribution based upon the dimension δ and the maximum local velocity U_m; the amplitudes were normalized using $U_m^6\ \delta\ W_{1/2}$. The normalized spectra* are shown in Figure 6 for each of the three flow regimes. Grosche [Reference 7] reports measurements made on a similar apparatus using a slot nozzle of much greater aspect ratio (W/H = 23) than Hayden's (W/H = 10), but did not vary plate length to investigate dependence on δ or $W_{1/2}$. Grosche did however vary the exit velocity over a wide range and his data may be used for comparison with that reported by Hayden and Chanaud. Figure 7 compares a normalized curve obtained from Grosche's sound pressure and mean flow measurements (taken at a free field observation point similar to Hayden's) when the slot nozzle was issuing exactly tangential to the plate; the trailing edge was in the "characteristic decay"

---

*The spectra are reported in terms of power although only free-field measurements were taken; the conversion process is based upon directivity considerations reported below.

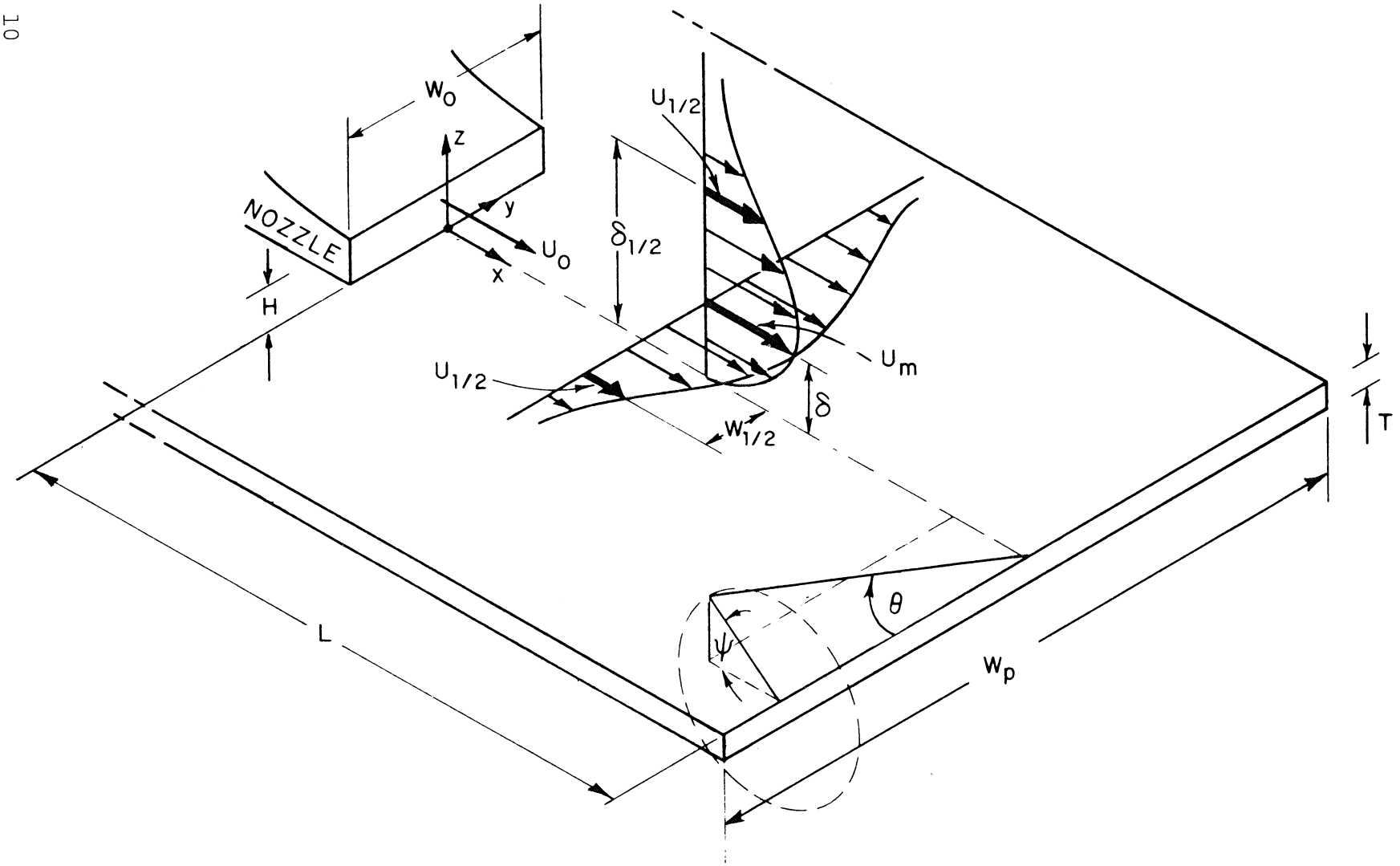

FIG. 4. COORDINATE SYSTEM AND TERMINOLOGY

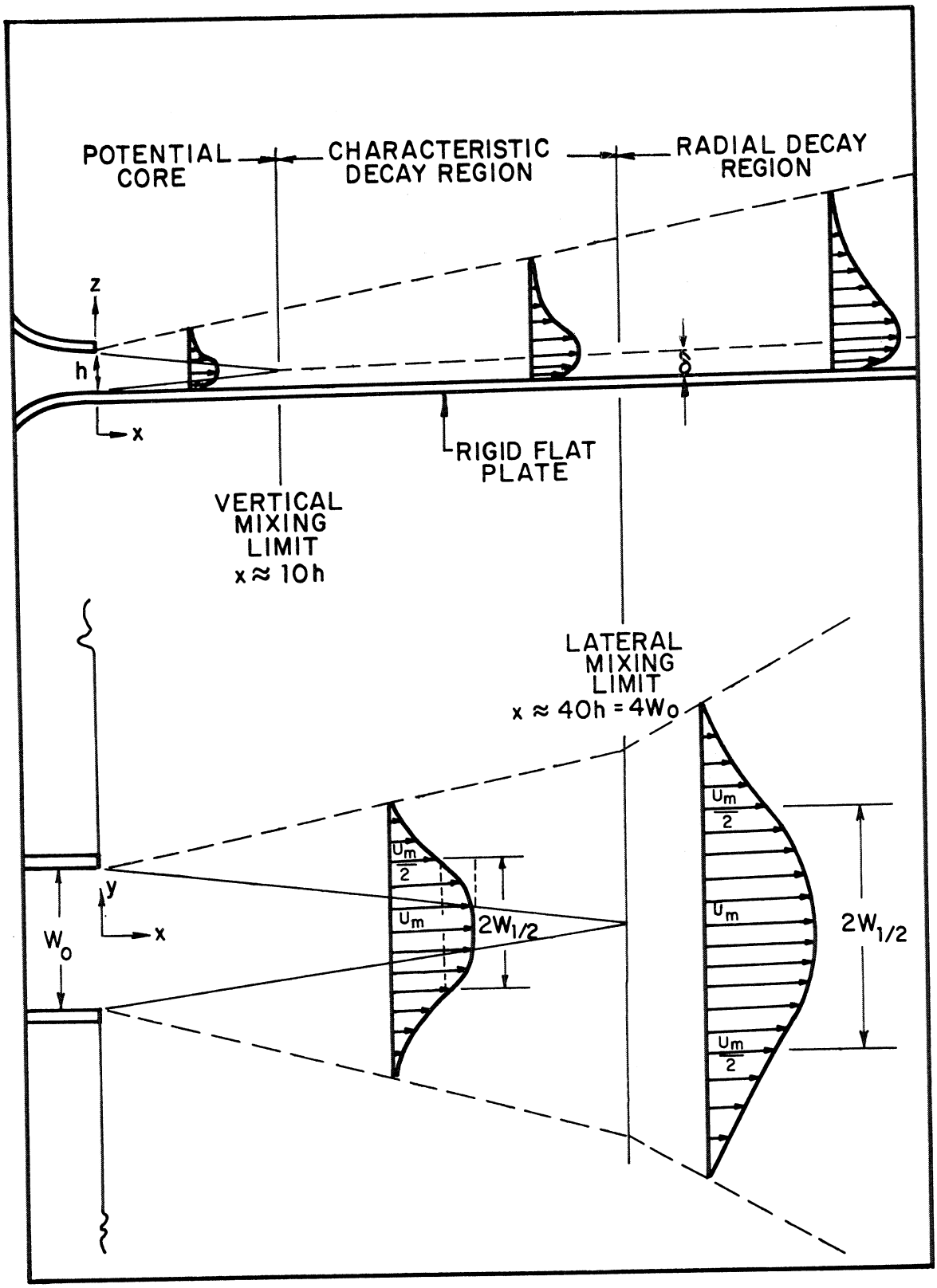

FIG. 5. THREE-DIMENSIONAL WALL JET CHARACTERISTICS

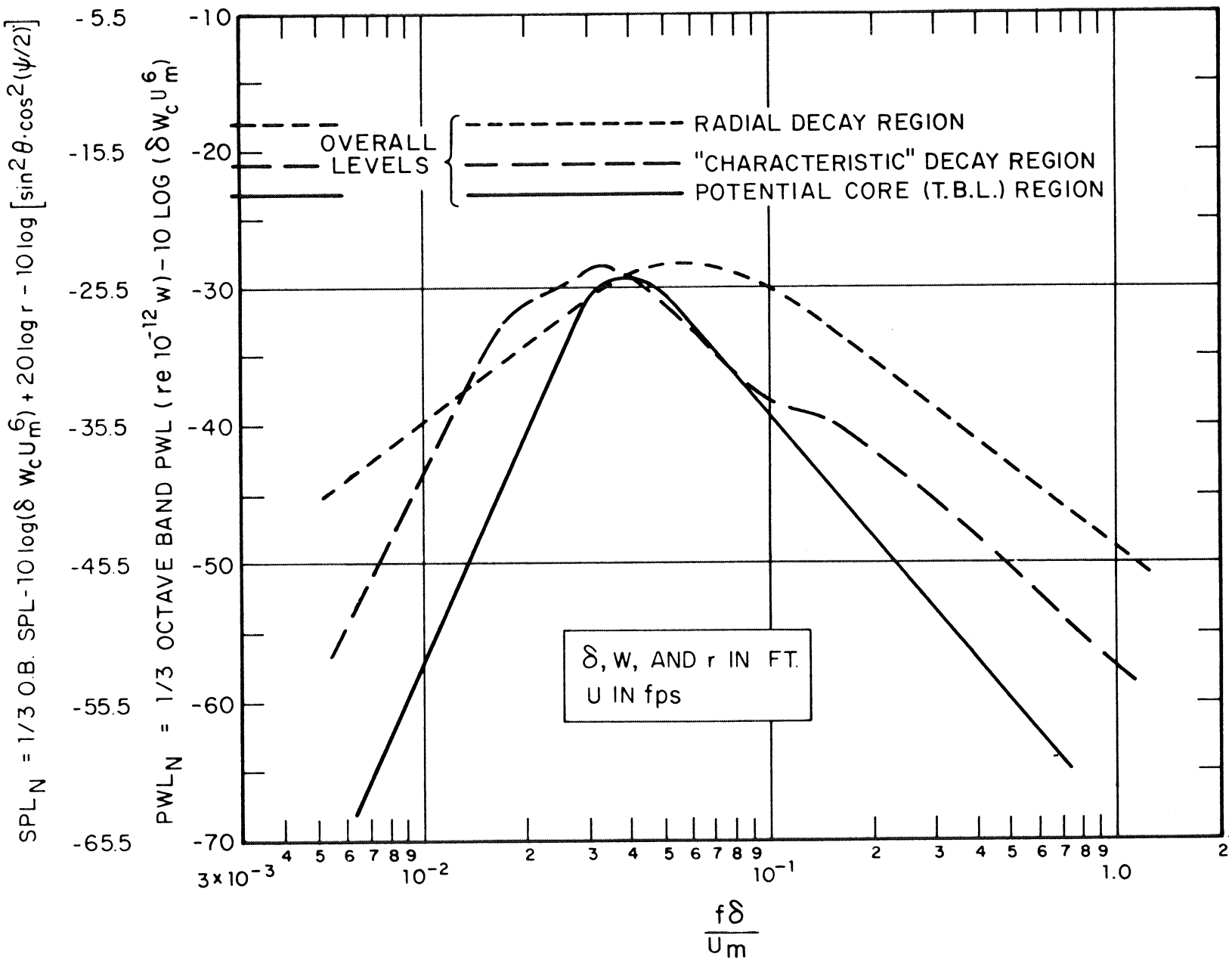

FIG. 6. NORMALIZED 1/3 OCTAVE BAND SPECTRA OF TRAILING EDGE NOISE

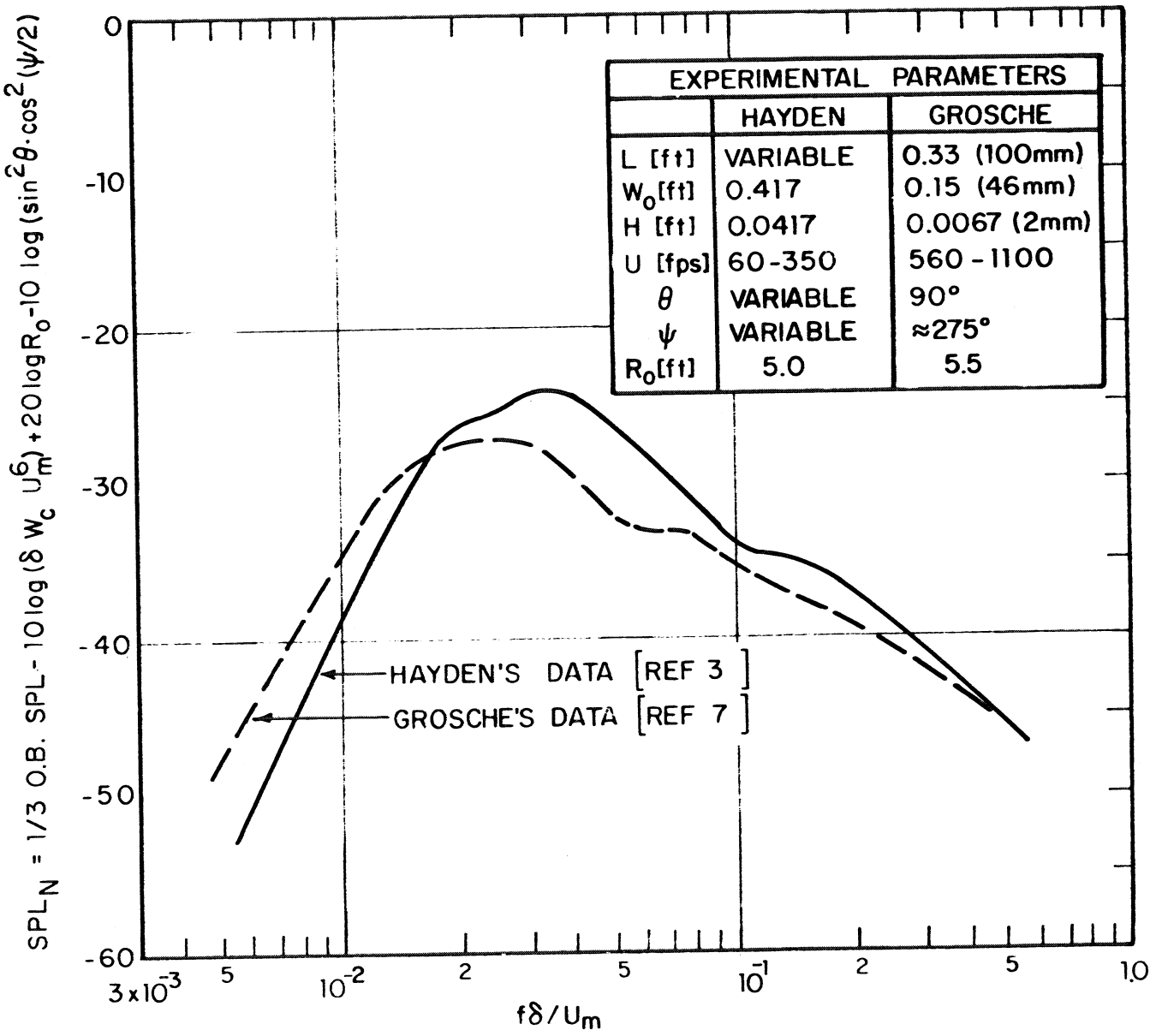

FIG. 7. COMPARISON OF TRAILING EDGE NOISE DATA

region in both cases. The agreement is quite good considering possible differences in flow field, and ratio of edge thickness to boundary layer thickness (which will be shown below to have some significance in total radiated sound power).

Directivity of the Edge Source. In cases where the acoustic wavelength of the edge sound is not large with respect to the upstream surface (assuming that there is no downstream surface in the neighborhood of the source), the directivity pattern of the resulting sound field is markedly different from that of the classical free field point dipole, such as described by Curle [Reference 6].

In this sense, the edge may be regarded as a partial baffle. Hayden and Chanaud [References 3,4,5] observed experimentally the "diffracted" nature of the trailing edge dipole and, using results of an earlier study of diffracting by wedges [Reference 8], were able to predict the limiting case where the "diffracting" surface is a semi-infinite plate of zero thickness.

The spatial distribution of mean-square sound pressure is described by

$$\overline{p^2}\ (r,\theta,\psi) \propto \frac{1}{r^2}\ \sin^2\theta\ \cos^2\left(\frac{\psi}{2}\right) \qquad (4)$$

using the geometry defined in Figure 4. The equal intensity level contours in several planes are shown in Figures 8(a) - 8 (c). This directivity pattern has been observed in situations when $kL \geq 1$; at lower kL values, the cardiod shape begins to return to the point-dipole-like directivity.

Effect of Edge Thickness. The total amount of acoustic radiation from turbulent flow past a trailing edge has been found to be a function of edge thickness - radiated *power**

---

*The presence of a thick edge modifies the directivity pattern from that described by Eq. 4, so free-field observations at a particular point may not reflect the reduction in sound level with increasing edge thickness.

(In all cases, $Kr >> 1$, $Kw_c >> 1$, $KL > 1$)

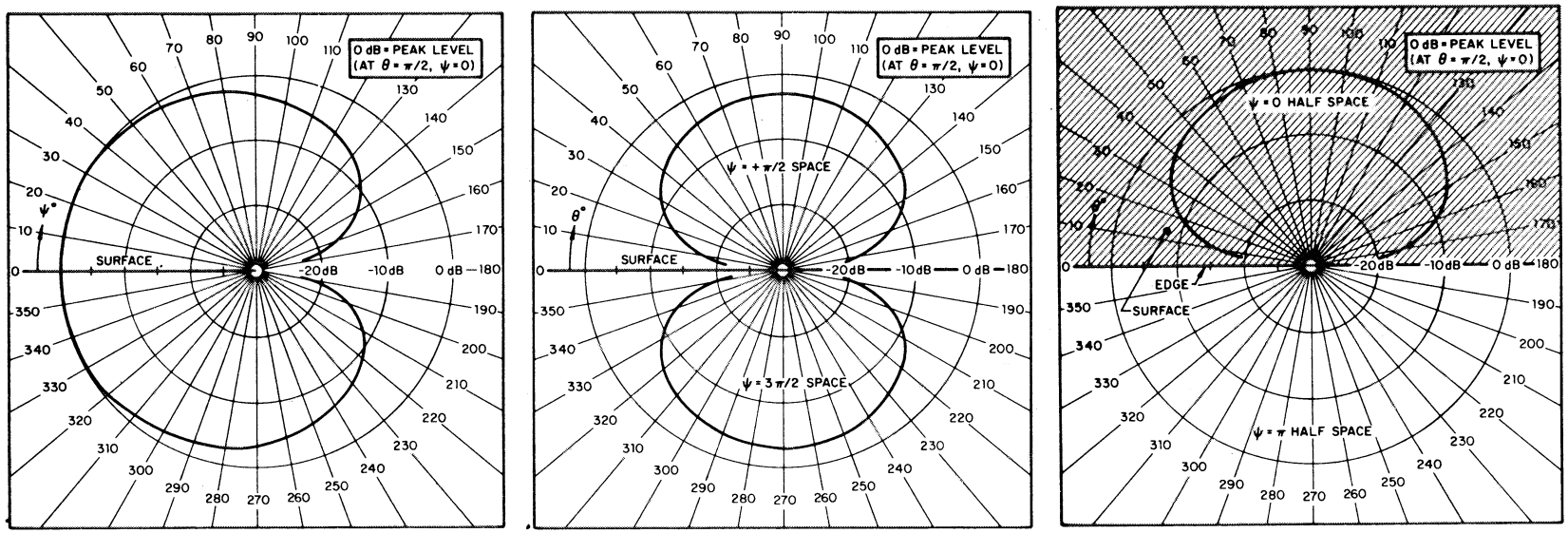

(a) In plane normal to surface and to span

(b) In plane normal to surface and parallel to span

(c) In plane of the surface

FIG. 8. DIRECTIVITY OF TRAILING EDGE NOISE SOURCE WHEN KL > 1

decreasing with increasing edge thickness. Typical variations observed [Reference 9] are shown in Fig. 9.

Edge Noise from Slot Nozzle/Plate Systems. Since the source model presented in Eq. 3 was verified experimentally, one can reinterpret the results to predict variation in overall sound pressure (or power) as a function of edge distance from a given nozzle (plate length). That is, the mean square sound pressure at a given position relative to the edge is

$$\overline{p^2\ (L/H)} \propto \left[U_m\left(\frac{L}{H}\right)\right]^6 \cdot \left[\delta\left(\frac{L}{H}\right)\right]^1 \left[W_c\left(\frac{L}{H}\right)\right]^1$$

For the three-dimensional wall jet flow field studied by Hayden and Chanaud, the following variations in U_m, δ and W_c were observed: ($W_c = W_{1/2}$ here):

Flow Regime:	Core $\left(o<\frac{L}{H}<12\right)$	Characteristic Decay $\left(12 \lesssim \frac{L}{H} \lesssim 40\right)$	Radial Decay $\left(\frac{L}{H} > 40\right)$
$U_m(L/H) \propto$	$(L/H)^{0}$	$(L/H)^{-0.36}$	$(L/H)^{-0.8}$
$\delta\ (L/H) \propto$	$(L/H)^{0.8}$	$(L/H)^{1.0}$	$(L/H)^{1.0}$
$W_{1/2}\ (L/H) \propto$	$(L/H)^{0.082}$	$(L/H)^{0.224}$	$(L/H)^{0.82}$

The predicted variation in mean-square pressure at a point relative to the edge is then:

Core: $$\overline{p^2\ \left(\frac{L}{H}\right)} \propto \left(\left(\frac{L}{H}\right)^0\right)^6 \cdot \left(\left(\frac{L}{H}\right)^{0.8}\right)^1 \cdot \left(\left(\frac{L}{H}\right)^{.082}\right)^1 = \left(\frac{L}{H}\right)^{0.88}$$

Characteristic Decay: $$\overline{p^2\ \left(\frac{L}{H}\right)} \propto \left(\left(\frac{L}{H}\right)^{-0.36}\right)^6 \left(\left(\frac{L}{H}\right)^1\right)^1 \left(\left(\frac{L}{H}\right)^{0.224}\right)^1 = \left(\frac{L}{H}\right)^{-0.94}$$

Radial Decay: $$\overline{p^2\left(\frac{L}{H}\right)} \propto \left(\left(\frac{L}{H}\right)^{-0.8}\right)^6 \cdot \left(\left(\frac{L}{H}\right)^1\right)^1 \cdot \left(\left(\frac{L}{H}\right)^{0.82}\right)^1 = \left(\frac{L}{H}\right)^{-3.0}$$

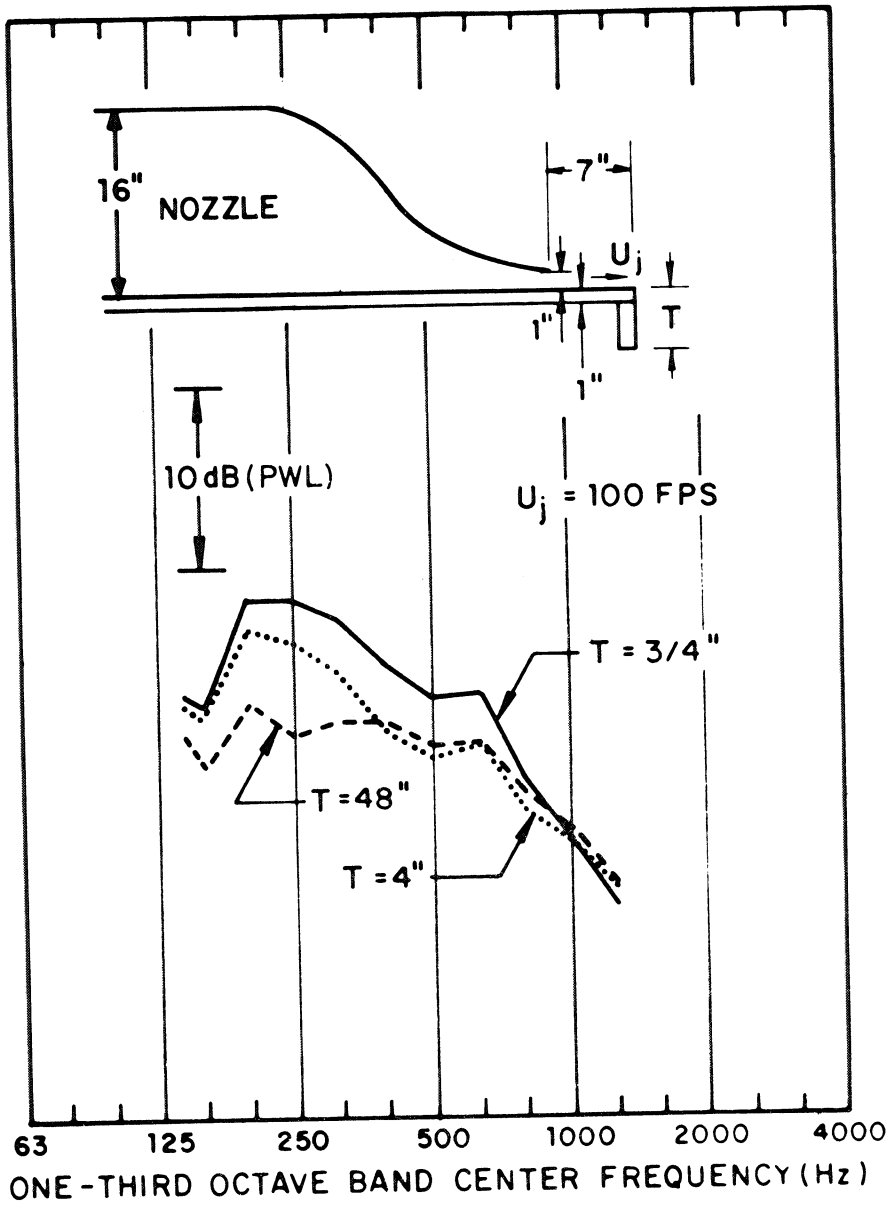

FIG. 9. OBSERVED REDUCTION OF "EDGE SOUND POWER" DUE TO EDGE THICKNESS [REFERENCE 9]

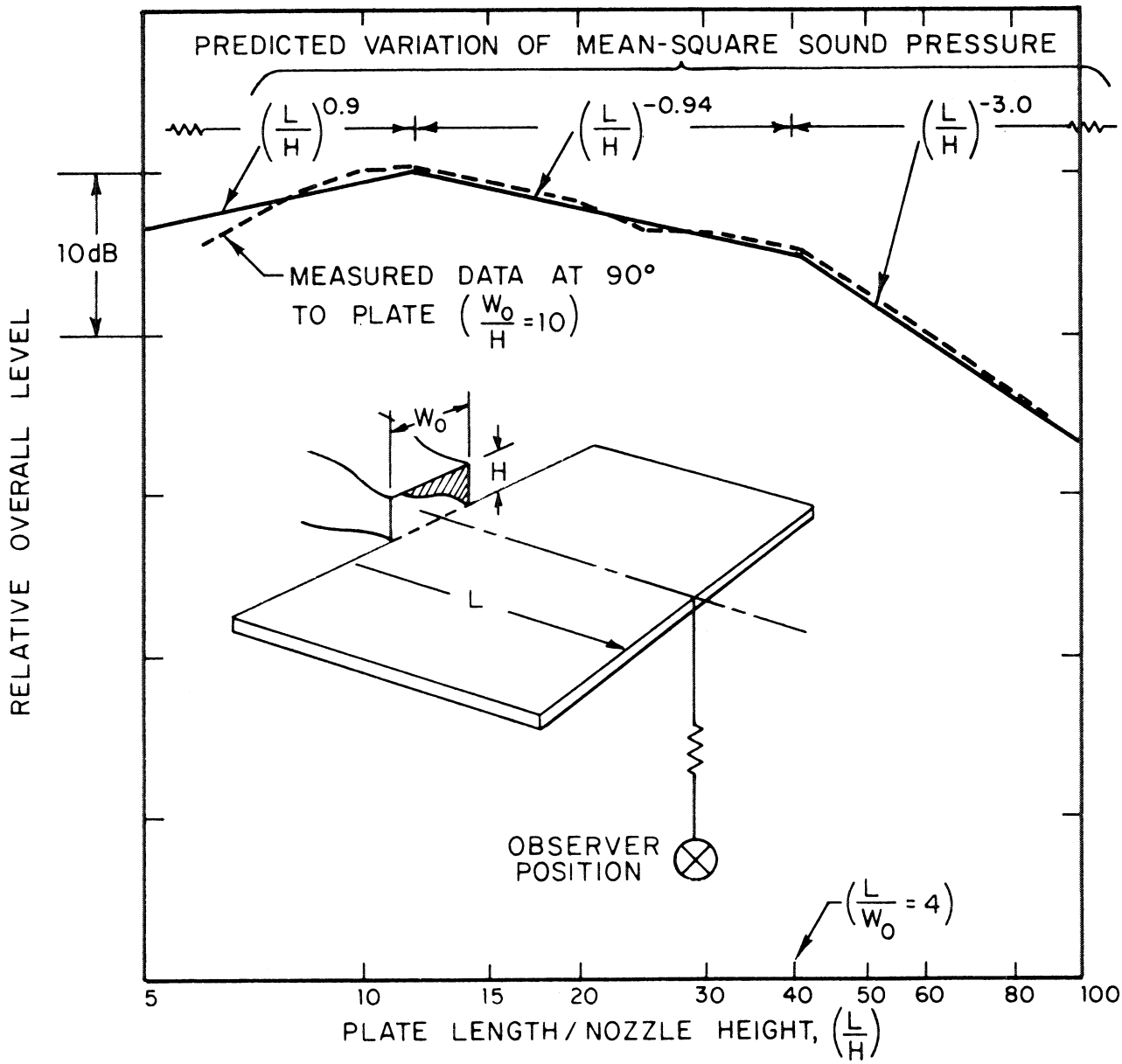

FIG. 10. TRAILING EDGE NOISE FROM A THREE-DIMENSIONAL NOZZLE/PLATE SYSTEM

These predictions are compared with experimental data in Fig. 10. For two-dimensional nozzles and wall jets, there is no equivalent to the radial decay region, and the overall levels would simply continue to fall off at approximately 3 dB per doubling of (L/H). It should be noted that $U_m(L/H)$ is somewhat dependent on the nozzle/plate configuration and considerable variation in the rate of change of U_m with (L/H) has been reported [Reference 3]. Since $\overline{p^2}(L/H)$ is so strongly dependent upon $U_m(L/H)$, one should expect considerable variation from the above predictions for generalized cases.

Flow on Both Sides of an Edge

Attention is now directed to the case of turbulent attached flow on both sides of a thin rigid surface. The question here is the following: "How will two statistically identical random pressure fields interact to produce sound when convected past opposite sides of the same edge?" The answer to this question is not straightforward. Part of the answer lies in the phase coherence information for the particular case of interest. Namely, if the pressures from the opposite sides of the edge were fully correlated then one would expect complete cancellation at the edge; if the pressures were negatively correlated, then the hydrodynamic force on the medium would increase over the single-sided case and thus more sound would be produced; finally, if zero correlation exists, then one could approximate the net sound output by addition of two incoherent sources of equal strengths - i.e., an increase of 3 dB over the one-sided flow case.

This case has been studied experimentally by Chanaud and Hayden [Reference 5], using a wall-jet flow field on both sides of a thin (1/4 in.), rigid plate. The results as compared to the "single-sided" case may be simply stated as follows:

1. The same dependence on mean flow parameters was observed as in the "single-sided" flow situation.
2. The same directivity was observed as before.
3. The broadband portion of the spectrum was positively (although weakly) correlated from one side of the edge to the other at low frequencies and tended toward zero correlation at very high frequencies.
4. The overall sound power was never more than 1 dB greater than the "single-sided" case.

5. A narrow band sound was produced by the wake of the plate. This part of the sound spectrum also varied in level as U_m^6 and obeyed a Strouhal number relationship where the characteristic linear dimension is the wake thickness δ_w; it was found that δ_w is approximated by the sum of the edge thickness T and the boundary layer *displacement* thicknesses δ^* on either side of the edge ($\delta^* \approx \delta/8$). The spectral peak of the wake-generated noise was at a Strouhal number of $f\delta_w/U_m \approx 0.25$, with a harmonic evident at $f\delta_w/U_m \approx 0.5$. The discrete "wake-noise" tone most predominant in the potential core regime of the wall jet, although it was observable in other regimes. Figure 11 shows normalized data which could be used for predicting wake induced noise for flows in which there is no free-stream turbulence (i.e., laminar mean flow above a turbulent boundary layer or wall jet flow in the potential core regime). Application of this plot should be restricted to the conditions stated above and trailing edge Reynold's number ranges between 10^5-10^6 based upon free-stream velocity U_m and boundary layer thickness δ ($10^5 \lesssim U_m\delta/\nu \lesssim 10^6$).

Empirical Formulations

The theoretical considerations and experimental observations summarized above may be utilized in forming empirical relationships for prediction of sound radiation in similar physical situations. In applying these schemes, one must be certain to identify correctly the applicable geometric, acoustic, and aerodynamic regimes. Namely, the following conditions should be met if good agreement between observation and prediction is to be expected:

1. Applicable geometric/acoustic regime: $kL \gtrsim 1$ (or $kC \gtrsim 1$ using earlier notation).
2. Flow field should be like a planar wall jet or turbulent boundary layer with no pressure gradient (i.e., accuracy will diminish for surfaces with jets impinging at an angle of attack near an edge, or for t.b.l. flows over curved surfaces).
3. Edge should be rigid, thin, and not rounded or cut away.
4. For free-field observations, observer should be in the acoustic and geometric far field ($kr \gg 1$, $kW_c \gg 1$).

When one or more of these conditions are not met, variations from the predicted overall level, spectral, and spatial characteristics of the sound field should be expected.

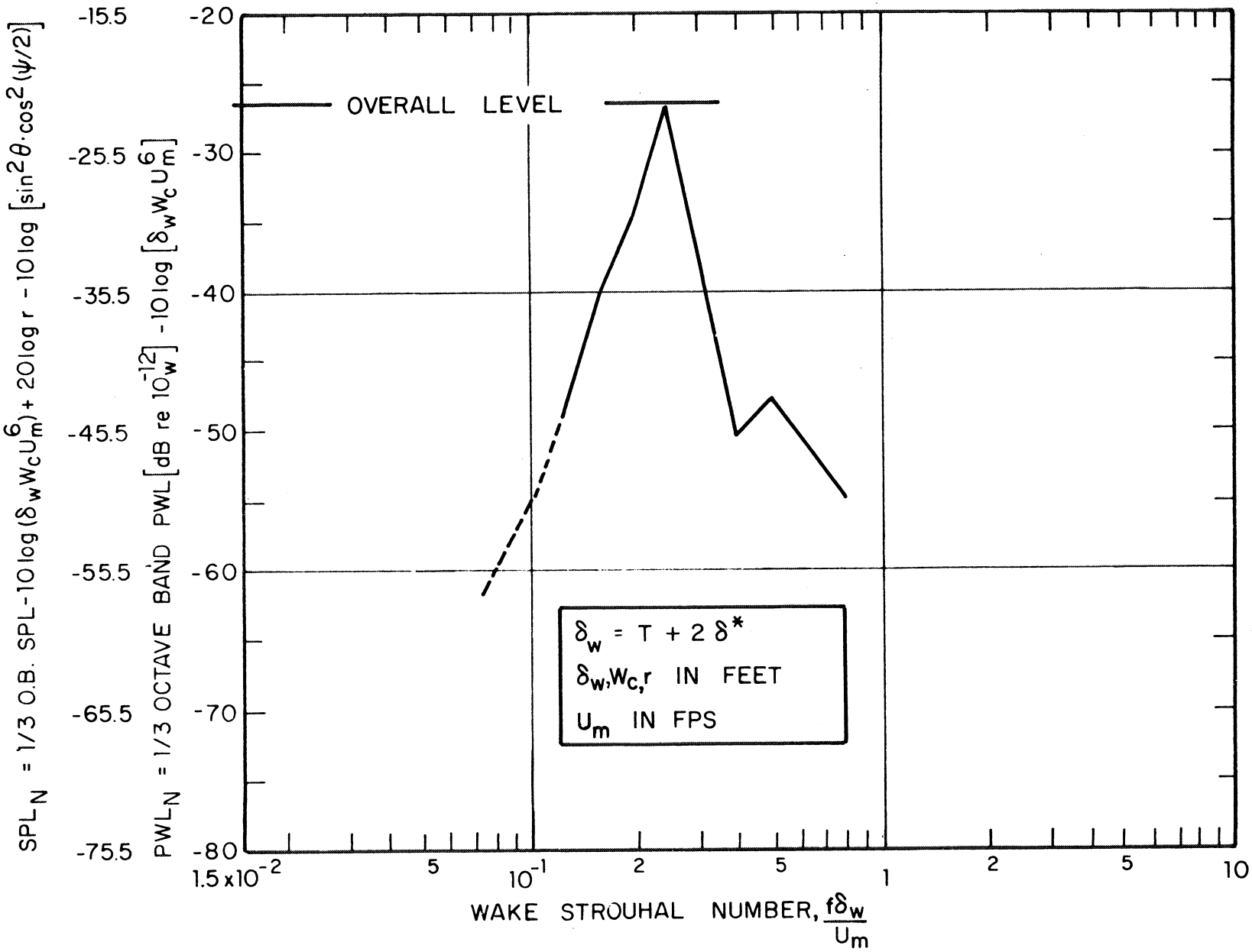

FIG. 11. NORMALIZED SPECTRUM OF WAKE-GENERATED NOISE; SEMI-INFINITE FLAT PLATE

Flow on One Side of Edge

Farfield Sound Pressure; Broad Band Component: (a) Overall SPL (dB re 0.0002 μbar) ($kr >> 1$, $kW_c >> 1$),

$$SPL_{OA}(r,\theta,\psi) = 10 \log(\delta W_c U_m^6) - 20 \log r + 10 \log[\sin^2(\theta)\cdot\cos^2(\psi/2)]$$

$$+ \begin{cases} -18.5 & \text{in wall jet core (or T.B.L.) region} \\ -16.5 & \text{in characteristic decay region} \\ -13.5 & \text{in radial decay region} \end{cases} \quad (5)$$

where units of r, δ, W_c are feet and of U_m are fps.

(b) One-third octave band spectrum levels relative to overall level. Compute overall level for appropriate flow field using Eq. 5; locate 1/3 O.B. Strouhal spectrum levels relative to overall using Fig. 6; compute actual frequencies from δ, U_m and Strouhal number values.

Sound Power. The sound power Π from a source may be determined from the integral over a sphere of the acoustic intensity I_r, where I_r may be approximated by the farfield mean square sound pressure divided by the characteristic impedance of the medium. Explicitly, in terms of earlier notation,

$$\Pi = \int_S I_r(r,\theta,\psi)\, dS$$

$$I_r(r,\theta,\psi) = \frac{\overline{p^2(r,\theta,\psi)}}{\rho c_o} \qquad \text{when } kr >> 1$$

For the trailing edge source,

$$\overline{p^2(r,\theta,\psi)} \propto \frac{1}{r^2} \sin^2\theta \cos^2(\psi/2) \quad (\text{when } kL >> 1).$$

Then, using an arbitrary reference observation point $r=R_o$, $\theta=\pi/2$, $\psi=\pi/2$, the sound power may be expressed in terms of the sound pressure at that point. For the source with the directivity pattern described above, the power is

$$\Pi = \frac{8\pi}{3} \cdot \frac{\overline{p^2\,(R_o, \pi/2, \pi/2)} \cdot R_o^2}{\rho c_o} \qquad (6)$$

Thus, the expressions for SPL can easily be converted to PWL

(a) Overall power level, PWL (dB re 10^{-12} w)

$$PWL_{OA} = 10 \log (\delta W_c U_m^6) + \begin{cases} -23 \text{ in wall jet core (or TBL) region} \\ -21 \text{ in characteristic decay region} \\ -18 \text{ in radial decay region} \end{cases} \qquad (7)$$

where units are the same as used previously.

(b) 1/3 octave band spectrum level relative to overall levels. Same procedure as (1b) again using Figure 6.

Equal Flow on Both Sides of a Thin Edge

Broadband Components: For both farfield sound pressure and sound power, use same procedure as above, but add +1 dB. ($\pm$1 dB is already considerably better accuracy than can be expected using the above techniques, due to small variations in flow fields, geometries, etc.)

Narrowband Wake-Generated Components: Accurate prediction of narrowband (wake-generated) spectra is much more precarious than prediction of the broad band component. In addition to the sensitivity of the fluid dynamical processes to small changes in surface condition, free-stream turbulence, and edge configuration, determining the exact bandwidth of this sound is difficult. The bandwidth of the radiated sound is, of course, dependent upon the bandwidth of the excitation which in turn is dependent upon the above-mentioned physical factors.

With these considerations in mind, the following prediction "scheme" is offered to be used in evaluating order-of-magnitude levels of wake-generated noise when the edge is immersed in a turbulent boundary layer beneath a turbulence-free mean flow, or under the potential core of a wall jet-like flow - and the δ-based Reynolds Number is in the vicinity of 10^5-10^6.

(a) Far Field SPL (dB re .0002 μbar) ($kr >> 1$; $kW_c >> 1$).

$$SPL_{OA}(r,\theta,\psi) = 10 \log[\delta_w W_c U_m^6] - 20 \log r + 10 \log[\sin^2\theta \cdot \cos^2(\psi/2)] - 22. \quad (8)$$

The 1/3 octave band spectrum can be determined by computing $f_{peak} = .25\ U_m/\delta_w$ and locating the rest of the spectrum with respect to this frequency and the peak level using Fig. 11.

(b) Power level (dB re 10^{-12} w)

$$PWL_{OA} = 10 \log[\delta_w W_c U_m^6] - 26.5 \quad (9)$$

The one-third octave band spectrum levels are computed in precisely the same manner as above, using Figure 11.

Illustrative Calculations

Arbitrary Case; Flat Plate in Smooth Flow. Consider a two-dimensional flat plate moving at zero incidence through air at 70°F at sea level. We wish to compute the radiated trailing edge noise sound power spectrum per unit span for the following conditions:

Forward speed, U_m:	300 fps	[91. m/s]
Chord plate length, L:	10 ft.	[3.3 m.]
Plate thickness, T:	1/4 in.	[.0068 m.]

To calculate the flow parameters, we use the standard relation for turbulent boundary thickness on a flat plate:

$$\frac{\delta}{x} = \frac{.22}{Re_x^{1/6}} \text{ which is applicable for } 10^6 < Re_x < 5 \cdot 10^8 \quad (10)$$

The length-based Reynold's number at the trailing edge is

$$Re_x = \frac{U_m x}{D}\bigg|_{x=L} = \frac{(300)(10)}{1.6\cdot 10^{-4}} = 1.875 \cdot 10^7 \qquad (11)$$

then δ_L = 2.2/16.4 = .134 ft [.044m.]. To calculate the broad band part of the spectrum, we use Eq. 7 recalling that 1 dB is added to account for the two-sided nature of the flow. The appropriate "normalization value" in that equation is -23 dB since the flow regime is "turbulent boundary layer". The overall power level is then

$$PWL_{OA}(\text{dB re } 10^{-12}\text{m.}) = -23+10 \log\left[(300)^6(.134)(1)\right]+1(\text{for 2-sided flow})$$

$$= 118 \text{ dB (per foot of span)}$$

Since it has been found [Reference 5] that the trailing edge noise model applies when KL > 1, then, for the 10 foot plate, the spectrum levels can be expected to be valid above about 20 to 30 Hz.

To compute the one-third octave band spectrum, an arbitrary Strouhal number is selected and the appropriate parameters substituted to locate the spectrum on the actual frequency scale. If the Strouhal number of the spectral peak ($f\delta/U_m = 4\times10^{-2}$) is selected, then the corresponding frequency is

$$f_p = 4\times10^{-2}\ \frac{U_m}{\delta} = \frac{(4\times10^{-2})(3\times10^2)}{.134} = 90 \text{ Hz.}$$

The spectrum is then easily located with respect to the overall level and is plotted in Figure 12.

Let us now compute the narrow band portion of the spectrum from Eq. 9. The Reynolds number is

$$Re_\delta = \frac{(300)(.134)}{1.6\cdot 10^{-4}} = .24 \cdot 10^6$$

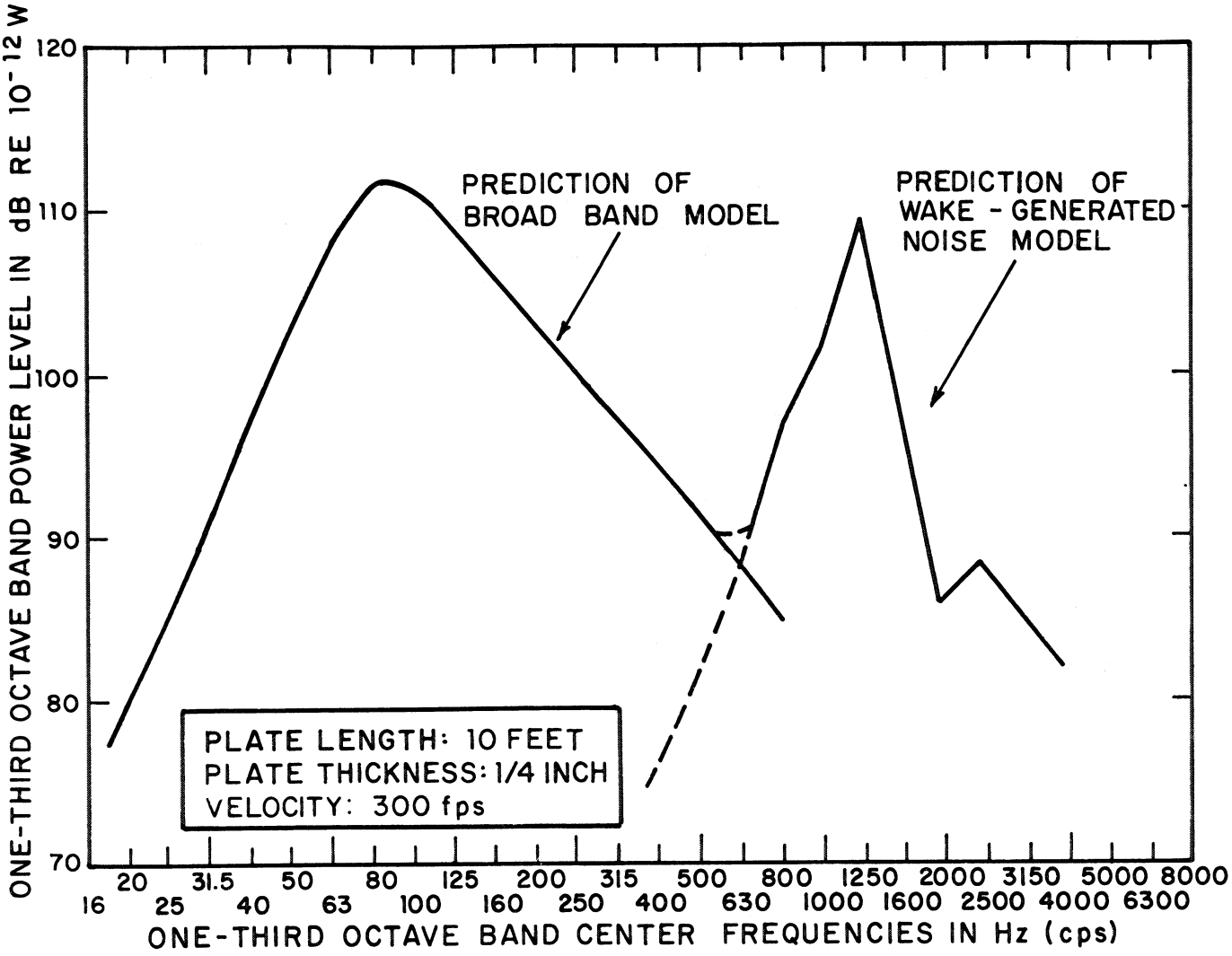

FIG. 12. CALCULATION OF TRAILING EDGE NOISE FROM A THIN FLAT PLATE MOVING IN STILL AIR AT 300 fps

which is within the valid Reynold's number range of data shown in Fig. 11. The wake thickness δ_w is $\delta_w = T + 2\delta^*$ (again assuming that the flow fields on either side of the edge are similar). δ^* may be approximated by $\delta/8$.

$$\delta^* = \frac{.134}{8} = .0168 \text{ ft}$$

Therefore, $\delta_w = .0546$ ft. The overall PWL (re 10^{-12} w) per foot of span is

$$PWL_{OA} = -26.5 + 10 \log [(300)^6 (.0546) (1)]$$

$$= 110 \text{ dB re } 10^{-12} \text{ w.}$$

The Strouhal peak of this spectrum is at $f\delta_w/U_m = .25$ which given a peak frequency of about 1300 Hz. This spectrum is also plotted in Fig. 12.

Comparison of Prediction with Measured Data. The sound power due to a airfoil section (NACA 0012) in smooth mean flow was measured in a free jet acoustic wind tunnel* [Reference 10]; these measurements can be used to test the prediction schemes developed previously for "trailing edge" and wake-generated noise. In addition to measurements of sound power (made in 1/3 octave bands), measurements of boundary layer and wake velocity profiles were made.

The relevant data is listed below:

NACA 0012 Airfoil
Chord Length: 6 inches
Wetted Span: 16 inches
Free Stream Velocity: 100 fps.
Angle of Attack: +4°
Boundary Layer Thickness at Trailing Edge: $\delta \approx .01$ ft.
Wake Thickness: $\delta_w \approx .0167$ ft.

*The wind tunnel had a low turbulence inlet contraction section (with a 16 in. x 16 in. opening) surrounded by a semi-reverberant room.

The prediction broad band power level is made using Eq. 7 together with the relevant physical parameters:

$$PWL(\text{dB re } 10^{-12}\text{w}) = -22+10 \log[(100)^6(10^{-2})(1.33)] = 79 \text{ dB}.$$

where 1 dB has been added to account for the "two-sided" flow.

The spectrum, valid for KL > 1 (f > 360 Hz), is determined in the same manner as in the previous example and is compared with measured data* in Figure 13. Reasonably good agreement is found above 360 Hz and even below that frequency, agreement is good considering that the airfoil was at a slight angle of attack and that the boundary layer was probably not fully developed (the length-based Reynolds number is not far from the critical number for transition to turbulence on a flat plate).

The δ-based Reynolds Number at the trailing edge is 0.63×10^4 which is considerably below the range of Reynolds numbers over which Eq. 9 and the data in Fig. 11 are valid. However, an estimate using these available techniques should prove informative.

The wake-generated peak is computed using Eq. 9:

$$PWL_{OA}(\text{dB re } 10^{-12}\text{w}) = -26.5+10\log [(100)^6(1.67\times10^{-2})(1.33)]=77\text{dB}$$

The frequency corresponding to the Strouhal number of the spectral peak ($f\delta_w/U_m = .25$) is 1500 Hz, (which is in the 1600 Hz band). The spectrum is determined in the usual way and is also plotted in Fig. 13. The prediction underestimates the observed levels (which were quite sensitive to small changes in surface roughness and small angle of attack variations) by 5 - 10 dB. The reason for disagreement would seem to be related

---

*There are two curves in Figure 13 for broadband sound power; the subject of Reference 10 was to investigate the use of modified leading edge structures - "serrations" - for reduction of noise from airfoils. As is evident in Fig. 13 the serrations removed the discrete frequency component but slightly increased the broad band component for the particular case treated here.

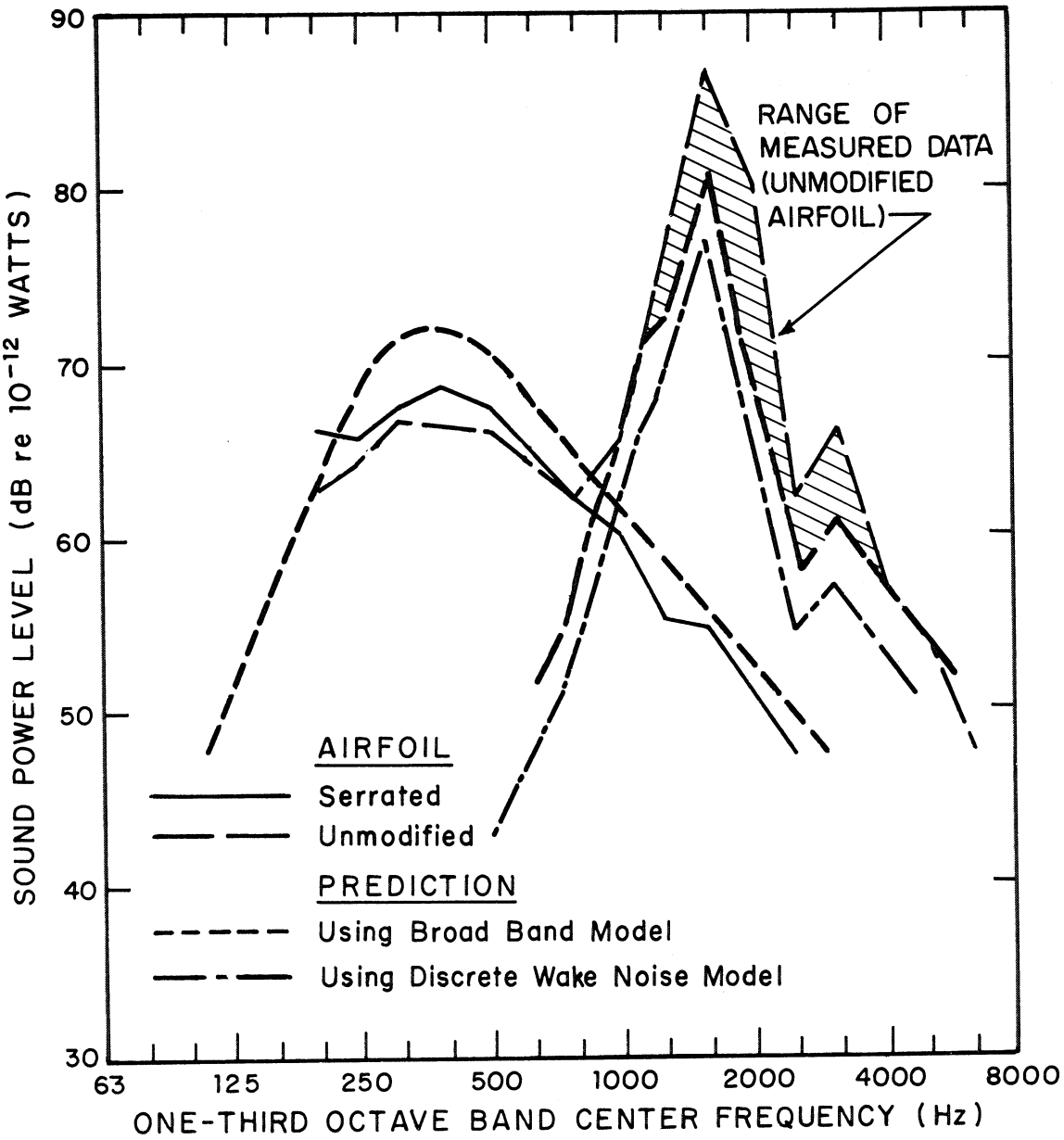

FIG. 13. COMPARISON OF PREDICTED AIRFOIL NOISE SPECTRUM WITH MEASUREMENT

to the crucial Reynolds number question and perhaps to the details of the trailing edge geometry - rounded [Reference 10] vs square [References 3-5]. However, this exercise illustrates the uncertainties still prevalent in the current understanding of the phenomena.

SOUND RADIATION BY RIGID BODIES IN DISTURBED INFLOWS

We now consider sound production by surfaces of finite dimensions which are immersed in unsteady inflows, such as airfoils operating in turbulence. This subject has received considerable attention, since a substantial part of the noise produced by aircraft compressor and fan blades is due to the unsteady aerodynamic forces induced on the blades by the upstream disturbances. However, in spite of all this activity, there still exists no coherent, experimentally verified theory which enables one to predict accurately sound production from an arbitrarily shaped body in an arbitrary inflow. There are perhaps several explanations for this problem, some of which will be given below.

General Discussion of Source Characteristics

The notion that solid bodies immersed in airflow radiate sound as a consequence of the unsteady forces acting upon them is due to Curle [Reference 6], who postulated that the sound pressure is proportional to the time rate of change of the aerodynamic force; namely, the sound pressure $p(r,t)$ is related to the force by

$$\overline{p^2(r,t)} \propto (1/r^2) \overline{[(\partial F)/(\partial t)]^2}$$

Curle's theory has been investigated through measurement of body forces and sound pressures and through measurement of directivity pattern (which is described by $\cos^2\theta$ where θ is the angle from the force axis). Unfried [Reference 11] was the first* to measure both applied force and farfield sound pressure characteristics. Unfried found excellent correlation between measured sound pressure field and that predicted from measured forces; his results were reported by Powell [Reference 12] in a treatise on "leading-edge tones". Sharland [Reference 13] found good agreement between experiment and Curle's theory for a small flat plate in large scale

*Several investigators had previously measured acoustic output from airflow over cylindrical wires and rods, finding that the dipole-like directivity pattern resulted in those cases. Curle's theory properly explains sound pressure patterns and levels from "Aeolian tones" - vortex shedding noise from cylinders - and for "leading edge tones". However, these subjects are outside the scope of this report and will not be discussed further.

turbulent flow. Heller and Widnall [Reference 14] utilized Sharland's interpretation of Curle's theory to perform experiments on flow spoilers wherein fluctuating forces were measured directly as was the resultant sound radiation. Heller and Widnall confirmed that sound power radiated from flow spoilers whose dimensions are *small* in comparison with an acoustic wavelength does vary in proportion to the mean-square force times the square of the characteristic frequency of that force. By way of explicit confirmation of this "long wavelength" theory, Clark and Ribner [Reference 15] performed a cross-correlation between measured lift fluctuations on an airfoil in a turbulent jet and the farfield sound pressure and found that the sound was in fact directly related to the fluctuating force. As was shown in the previous section, the aerodynamic force is related to the square of the flow velocity, and the frequency to the first power of velocity; thus the mean square of this product gives the familiar U^6 dependence of the overall sound power. However, none of the studies mentioned to this point provide directly sufficient information to calculate accurately radiated sound levels without first measuring forces on the body of interest. Herein lies one of the key problems in prediction of sound from bodies in turbulent inflows - accurate calculation of the aerodynamic force spectral density from aerodynamic and geometric parameters alone.

The subject of airfoil response to unsteady inflows is one having been treated rather extensively in aeroelasticity texts [References 16-21], from which considerable guidance can be derived toward predicting sound radiation. However, the acoustical aspect of the problem is complicated by the fact that as the body becomes increasingly sizeable, it no longer may be modeled as a point source. Thus, one may be able to predict forces on an airfoil in turbulence, but his acoustic model may no longer be valid in that wavelength/body dimension regime. Also, for large bodies and those at high subsonic Mach numbers, phase coherence and convection information becomes important to the accurate modeling of the sound source. With all these restrictions in mind, one might justifiably wonder whether or not any accurate predictions can be made. The answer lies in the ability to make reasonable approximations and to be aware of accuracy limitations in regimes outside the realm of valid approximation.

Several regimes are examined below for which some experimental evidence is available.

Sound from Airfoils in Turbulent Airflows. Consider the case of a rigid airfoil of chord C and span B immersed in a subsonic turbulent inflow. When the characteristic scale of the eddies is not small with respect to the chord length of the airfoil, then one may apply some form of quasi-steady argument to describe the lift fluctuations. Once the lift fluctuations are described, one may model the surface as a small (again, small with respect to a wavelength) spherical source and modify the point dipole expression to account for reduced radiation at the wavelength/body size ratios small with respect to the chord length.

Description of the sound source - The sound power per unit bandwidth of a spherical point dipole source may be written

$$\frac{\Pi(\omega)}{\Delta\omega=2\pi} = \frac{\Phi_F(\omega)\omega^2}{12\pi\rho\, c_0^3} \tag{12}$$

where $\Phi_F(\omega)$ is the force spectral density at the radian frequency ω, δ and c_0 have their usual meanings. To find spatial characteristics of the sound, one may account for finiteness of the source and arbitrary orientation of the source axis by the following expression for farfield sound pressure (see Fig. 14 for coordinate system).

$$\Phi_p(r,\theta,\psi,\omega) = \frac{\Phi_F(\omega)}{16\pi^2 r^2} \left(\frac{k^2}{1+k^2a^2}\right) \cdot D(\theta,\psi) \tag{13}$$

where k is the acoustic wavenumber = ω/c_0, a is the effective radius of the source, and $D(\theta,\psi)$ is the directivity factor given below:

$$D(\theta,\psi) = \cos^2\theta_s \cos^2\theta + 2\cos\theta_s \sin\theta_s \cos\theta \sin\theta \cos\psi + \sin^2\theta_s \sin^2\theta \cos^2\psi. \tag{14}$$

(Note that this simply reduces to the usual $\cos^2\theta$ dependence when the source axis is aligned with the z-axis.)

The shape of the directivity pattern is the figure eight shown in Fig. 15 where the maxima are along the force axis and minima exist in the plane normal to the force axis.

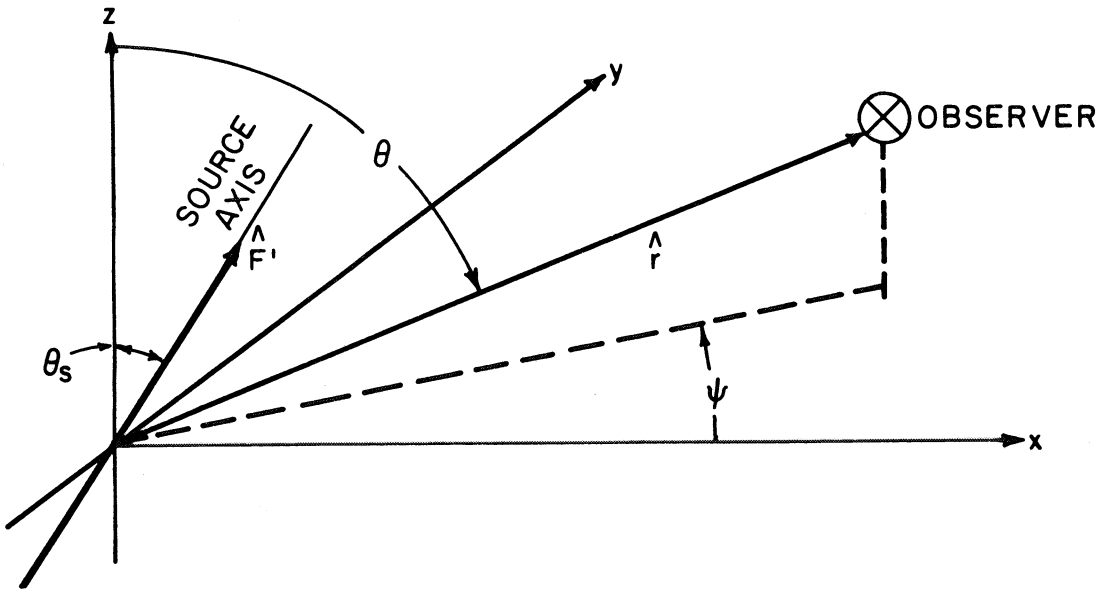

FIG. 14. COORDINATE SYSTEM FOR COMPUTING POINT DIPOLE SOUND FIELD

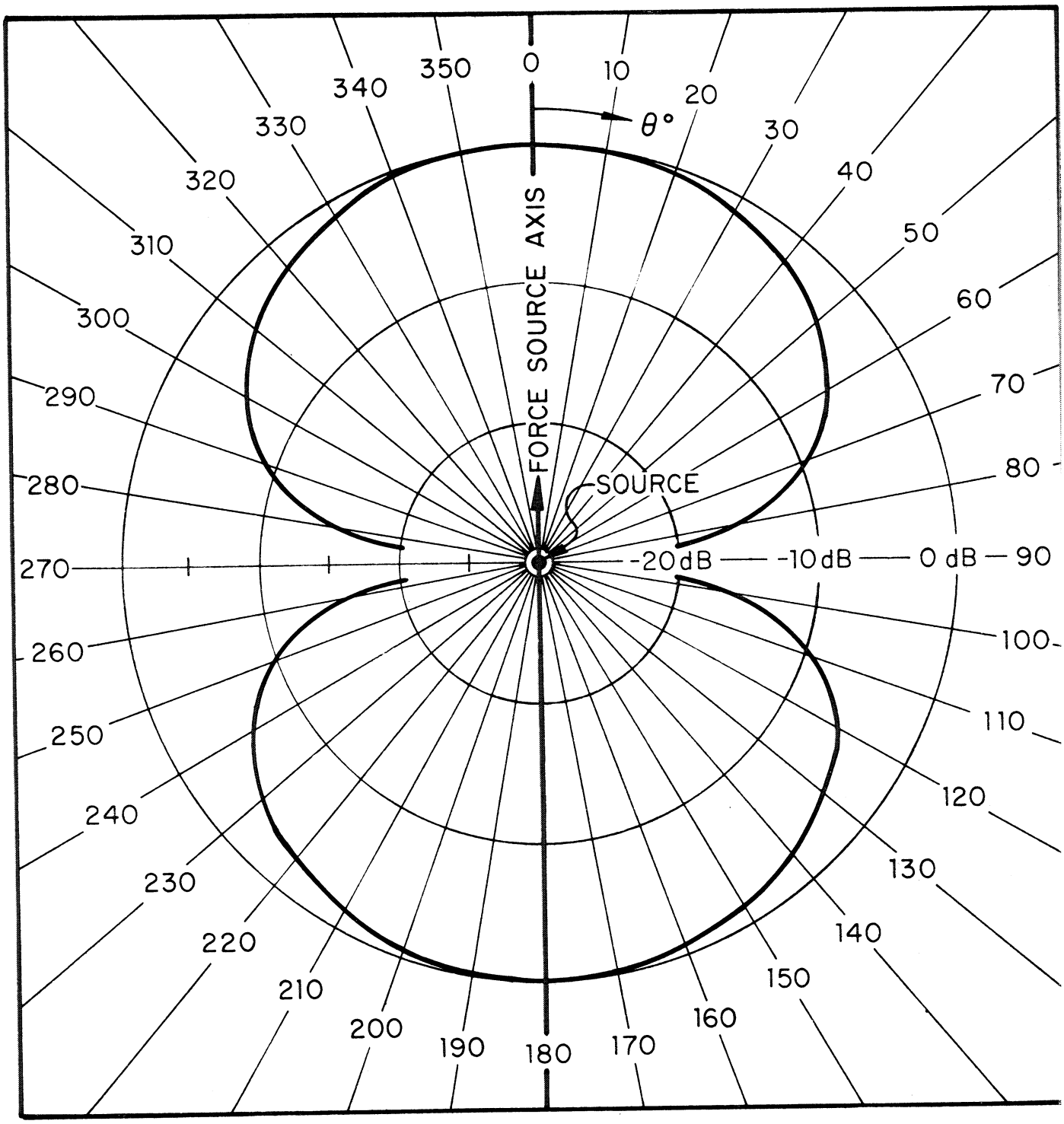

FIG. 15. SOUND PRESSURE LEVEL DIRECTIVITY FOR FREE-FIELD POINT DIPOLE

Lift Response of Airfoils in Two-Dimensional Inflows. Quasi-steady approximation - For the case of a two-dimensional airfoil in large-scale two-dimensional turbulence, the crudest approximation of the fluctuating (lift) force F_L' due to passage of a single eddy is the quasi-steady approach:

$$F_L' \approx C_{L_\alpha} \frac{1}{2} \rho U_m^2 A_c \left(\frac{w'}{U_m}\right) \tag{15}$$

where C_{L_α} is the steady-state lift curve slope*, U_m is the free stream velocity, A_c is the correlation area of the flow disturbance, $[w'/U_m]$ is the turbulence intensity in the direction normal to both the mean flow direction and the leading edge of the airfoil (i.e., "upwash intensity").

The characteristic frequency of the disturbances is directly proportional to the eddy convection speed and inversely proportional to the characteristic eddy scale δ_e. The frequency has been shown by Sharland [Reference 13] to be $\omega_c \approx U_m/\delta_e$ for a flat plate in jet turbulence (ω = radian frequency). With knowledge of the eddy scale and distribution, one may simply substitute Eqs. 14 and 15 into Eq. 13 to predict the sound pressure.

If the airfoil and upwash disturbance are not two-dimensional (they seldom are), but the spanwise mean velocity is uniform, then for lack of detailed information about the flow field one may apply the above analysis in strips across the span to deduce an approximation to the total lift response of the airfoil. The net sound power is then the incoherent sum of the sound power from each strip. Hayden [Reference 22] has found good agreement between experiment and the above method of prediction for a variety of lifting and bluff surfaces immersed in turbulent duct flow of a scale greater than the chord of the surfaces. However, the above approach is crude and restricted to low "reduced frequencies" ($\omega C/2U_m < .05$). Refined approaches are discussed below.

---

*The lift curve slope may be regarded as the transfer function between upwash disturbance w' and lift response of the airfoil.

The Sears' function approach - Considerable refinement on the quasi-steady approach may be made through the work initiated by von Karman and Sears [Reference 16] on airfoil response to unsteady inflows. A representative list of subsequent works includes Sears [Reference 17], Leipmann [Reference 18], Bisplinghoff [Reference 19], Filotas [Reference 20], and Theodorsen [Reference 21]. The Sears function represents the transfer function between sinusoidal upwash velocity fluctuations and resultant lift force fluctuations of the airfoil. In real time, the Sears function lift response to a sinusoidal upwash disturbance is

$$\frac{\dot{L}}{\text{unit span}} = \pi\rho C U_m^2 \left(\frac{W}{U_m}\right) e^{i\omega t}\, \Psi(k_x) \qquad (16)$$

where $\dot{L}$ is the unsteady lift at a particular reduced frequency

W/U_m is the magnitude of the upwash turbulence intensity

$\Psi(k_x)$ is the Sears function

k_x is the reduced frequency $= \frac{\omega C}{2U_m}$, (also called normalized chordwise wavenumber).

Sears [Reference 17] gives an expression for $\Psi(k_x)$ which is a complex quantity; the lift response is the real part of $\Psi(k_x)$ which has been represented by Bender [Reference 23] in polynomial form:

$$\frac{\dot{L}}{\text{unit span}} = \left[\frac{1.4k_x+1}{(1.4k_x^2+4.35k_x+1)}\right] \pi\rho C U_m^2 \frac{W}{U_m} . \qquad (17)$$

However, for real airfoils the above approaches must be further modified to account for finiteness of the airfoil ("end effects"). Bender [Reference 23] has recently shown that the finiteness correction for finite span airfoils (still for two-dimensional inflows) may be accurately approximated by multiplying Eq. 17 by the ratio of the steady-state "finite aspect ratio" lift curve slope to 2π (lift curve slope for infinite span thin airfoils). If the inflow is not two-dimensional, then the two-dimensional approximations given above will produce over-prediction of the lift response. Three-dimensional effects are examined below.

Lift Response of Airfoils in Three-Dimensional Inflows. Strip theory - If one has information concerning the spanwise distribution of eddy scale and phase, then the two-dimensional approaches may be applied in spanwise strips, the width of each strip being the eddy integral scale. Although the approach is conceptually sound, there is not a great deal of published information as to accuracy of the strip techniques; therefore, its validity cannot be further assessed here.

Integral approximation due to Mugridge - In a recent publication [Reference 24], Mugridge summarized a derivation from his thesis [Reference 25], of an approximate closed-form expression of lift response of a finite span thin airfoil to a convecting three-dimensional sinusoidal upwash. Qualitatively, Mugridge's solution shows a reduction of lift response at small values of turbulence wavenumber compared to the two-dimensional solution.

When the inflow has an upwash distribution that can be described by

$$w(x,y,t,\omega) = W\, e^{-\left[i\left(\omega t - \frac{\omega}{U_m}x + my\right)\right]},$$

the mean square lift response may be written

$$\overline{L^2(k_x,k_y)} = \rho^2 U_m^4 b^2 \pi^2 \left(\frac{W}{U_m}\right)^2 \left(\frac{1}{1+2\pi k_x}\right)\left(\frac{k_x^2 + 2/\pi^2}{k_x^2+2/\pi^2+k_y^2}\right)\left(\frac{\sin k_y}{k_y}\right)^2 \qquad (18)$$

where b is the span

W is the magnitude of the upwash disturbance

k_x is the normalized chordwise turbulence wavenumber = $\omega C/2U_m$

k_y is the normalized spanwise turbulence wavenumber = $mb/2$

To utilize fully Eq. 18, one must have detailed information about k_x and k_y or make approximations for very large k_y (net lift tending toward zero) or very small k_y (lift response tending toward two-dimensional solution).

If the upwash statistics are defined such that for every chordwise wavenumber k_x, there is a spanwise turbulence spectrum determined through an integral correlation length $L(k_x)$, one may obtain closed form expressions for the mean square lift for a finite span airfoil in three-dimensional inflow and a two-dimensional airflow ($k_y = 0$). Mugridge gives such expressions for the case where end effects are neglected [Reference 24]. These are summarized in Figure 16 where it may be observed that three-dimensional effects substantially reduce the airfoil response at low wavenumbers and high values of $b/L_w(k_x)$, but have little effect at high wavenumbers and low values of $b/L_w(k_x)$.

Dean [Reference 26] has found that Mugridge's result provides a good fit to measured acoustic data of a small airfoil in fully-described three-dimensional inflow where the source was assumed to be a point dipole.

Effect of Deviation from Point Dipole Regime

Despite the fact that prediction of lift response of airfoils is currently well-in-hand, prediction of sound from these airfoils when the "point source" criterion is not satisfied (i.e., when $kC > 1$) is not well understood or at least well confirmed experimentally. There is at least one study [Reference 5] which suggests that, for a thin plate (or airfoil) in a finite width turbulent inflow, a limiting value of acoustic output is reached when the trailing edge becomes distant from the leading edge (in terms of acoustic wavelengths). In this case, the directivity is modified from the point dipole case toward that observed for "trailing edge noise" on a semi-infinite surface. Since, in general, the inflow could be sufficiently uncorrelated along the leading edge span to cause nearly complete cancellation of net fluctuating forces on the airfoil, one expects that one could describe the sound field through a generically similar argument to the analogous trailing edge noise situation.

Empirical Formulations

No empirical formulations will be presented for predicting sound from bodies in disturbed inflow, since rather exact formulations are possible when one has information on force spectra. It has been shown that, in many cases, one may readily predict force spectra from inflow turbulence statistics. If this information is not available, then one may have to revert to much more approximate schemes such as presented in the next section.

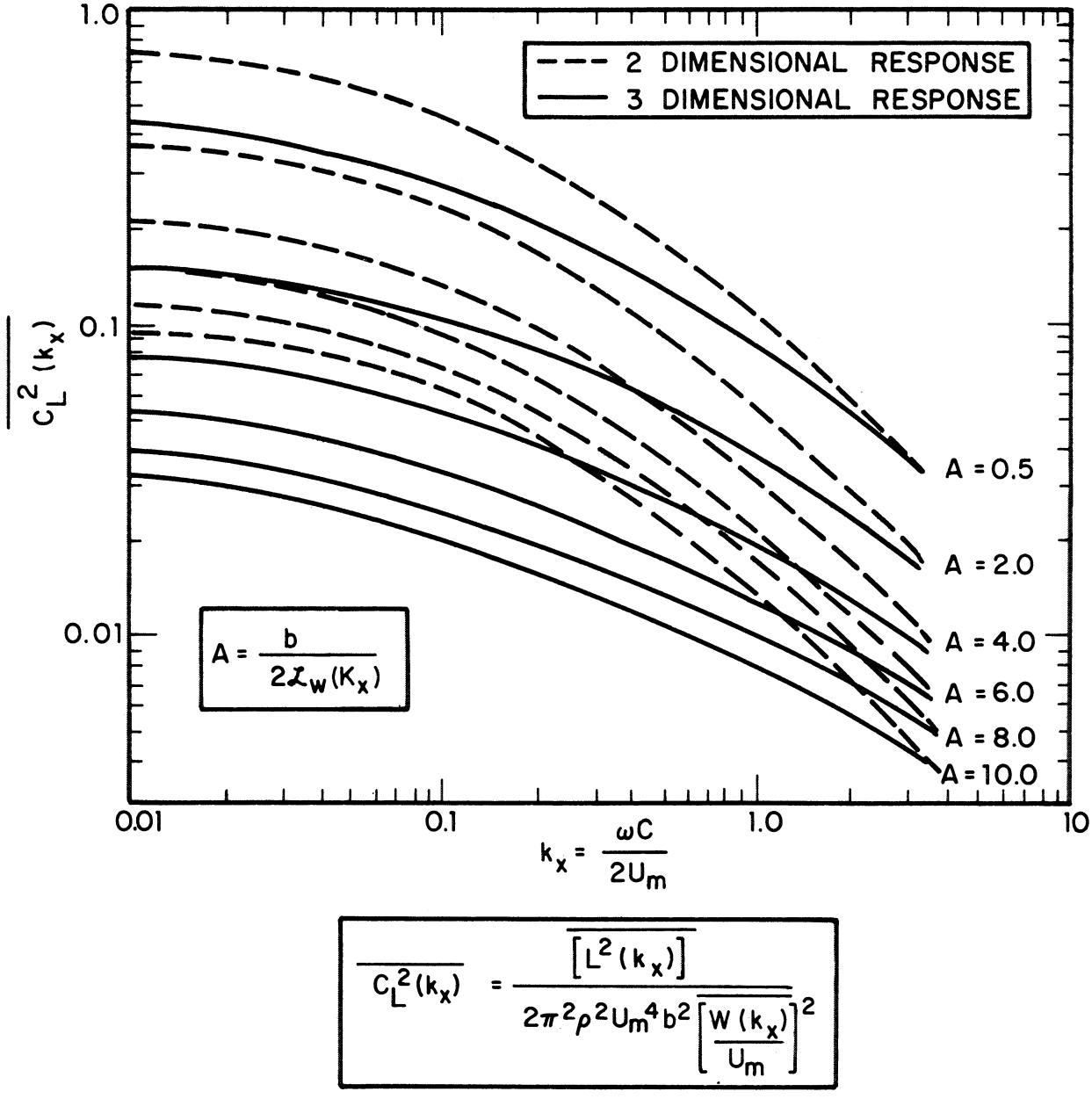

$$\overline{C_L^2(k_x)} = \frac{\overline{\left[L^2(k_x)\right]}}{2\pi^2\rho^2 U_m^4 b^2 \overline{\left[\frac{W(k_x)}{U_m}\right]}^2}$$

FIG. 16. LIFT RESPONSE OF FINITE SPAN AIRFOILS IN 2- AND 3-DIMENSIONAL INFLOWS

SOUND RADIATION FROM FLOW SPOILERS IN A CONFINED ENVIRONMENT

In this section we progress to an examination of sound from small, rigid bluff bodies placed inside a rigid flow duct. This is essentially a summary of the works of Heller and Widnall [Reference 14] and Gordon [Reference 27], who have developed from experimental data, accurate methods for predicting sound radiated into free field from the end of a rigid duct due to the presence of an upstream flow spoiler.

Theoretical Treatment

Flow spoiler in free-field environment. The radiated acoustic power of a small* "flow-spoiler" can be expressed in terms of the fluctuating force F, as

$$\Pi(\omega) = \frac{F^2(\omega)\cdot\omega^2}{12\pi\rho c_0^3} \qquad (19)$$

Here ω is the frequency and ρ and c_0 are the density and speed of sound, respectively.

Flow-spoiler in confined environment. Heller and Widnall [Reference 14] have shown that immersion of a flow spoiler into the confinement of an air duct (Fig. 17) alters its noise output. Their analysis evaluates changes in sound radiation from the end of a (spoiler-containing) hard-walled duct due to various placements of the spoiler with respect to the end of the duct. For the present, consider the case of $D < \lambda$ and $d < \lambda$, where D is the pipe diameter, λ is the acoustic wavelength, and d is a typical body dimension (Fig. 17). Thus, again the analyses are restricted to the case of the acoustic wavelength being much larger than the pipe diameter, so that the acoustic energy propagates as a plane wave, i.e., in a one-dimensional form along the pipe. The other requirement, that the spoiler is much smaller than the wavelength, permits one to treat the field in the neighborhood of the spoiler as essentially incompressible. From these restrictions, one can develop rather simple models for the various aerodynamic source types and straightforwardly determine the

---

*Small, in comparison with the characteristic acoustic wavelength (again $kd << 1$, where d is the characteristic dimension of the spoiler).

FIG. 17. SPOILER-IN-DUCT GEOMETRY

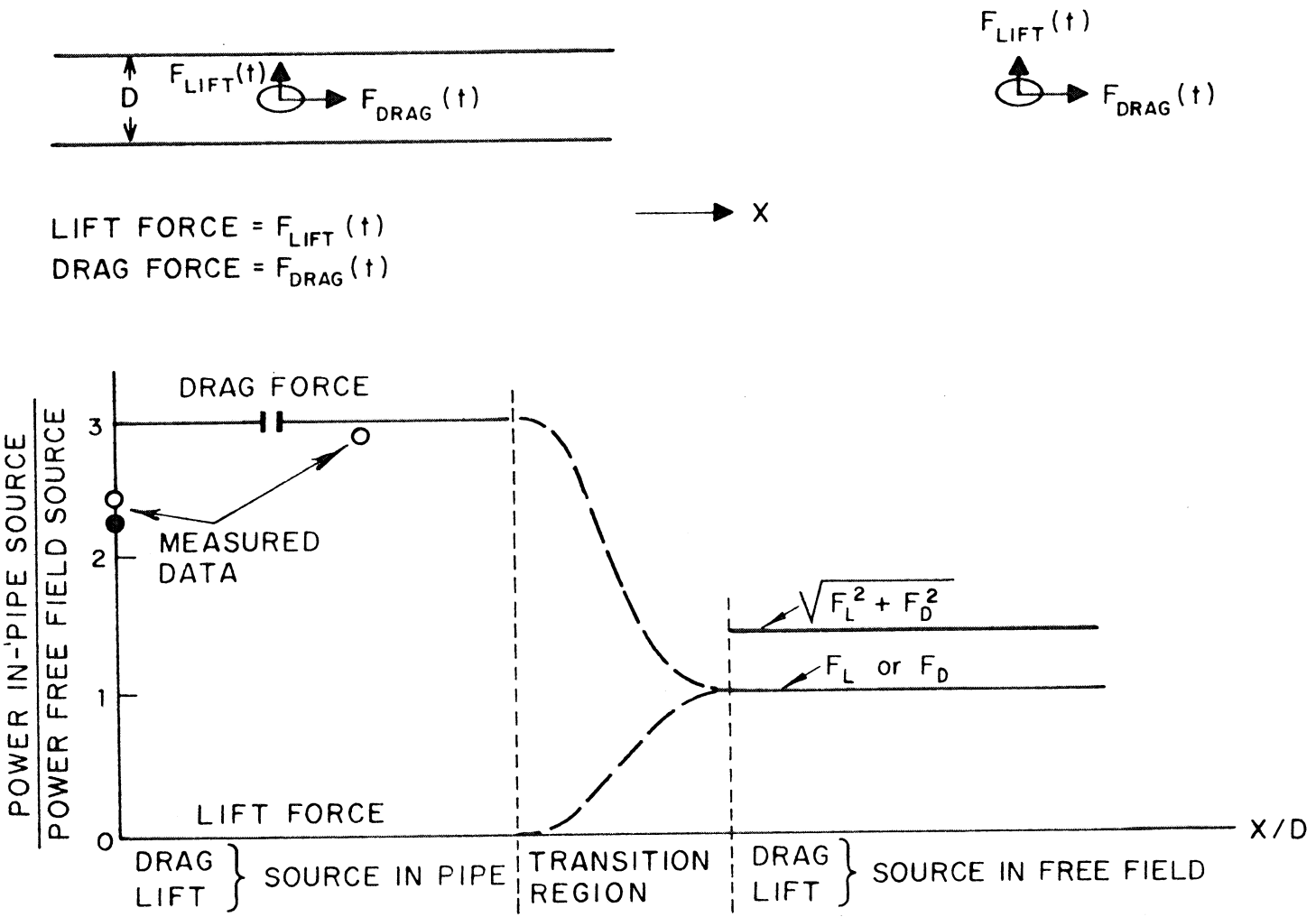

FIG. 18. CHANGE OF SOUND POWER OUTPUT FOR SPOILER SOURCE IN-DUCT AND FREE-FIELD

change in radiated power due to insertion into a semi-infinite pipe.

The analysis shows that the sound power observed in the free field beyond the pipe exit from a dipole source of strength F is given by

$$\Pi(\omega) = \frac{F^2(\omega)\ \omega^2}{4\pi\ \rho\ c_0^3}\ , \qquad (20)$$

which is a factor of 3 (or about 5 dB power level) more than what the same source radiates in a free field environment (Eq. 19).

Equation 20 is valid for sources located in the pipe a distance of at least one wavelength from the pipe exit. As a source is moved closer to the exit, and eventually out of the exit into the free field, a transition to the free-field case will occur. The proportionality between sound power observed in the free space beyond the pipe to source strength F changes from its in-pipe value to the free-field value in a transition region about the pipe exit. This change is *qualitatively* indicated in Fig. 18. Sound due to lift-force fluctuations cannot be observed in the free-field environment from an in-pipe source since lift forces in a pipe cancel, thus the proportionality constant goes to zero (neglecting diffraction).

The results indicate that an aerodynamic dipole source in a pipe-like confinement will always radiate in proportion to the sixth power of a typical flow velocity both at low and high frequencies. At low frequencies, however, dipole efficiency for an in-pipe source location is increased by a factor of 3 (~5 dB).

Empirical Formulations

In the previous section, formulations were presented for relating radiated sound power from aerodynamic dipoles to the fluctuating force magnitude. For a flow-spoiler system, such as shown in Fig. 17, it is quite tedious to calculate the force spectrum on the spoiler due to impinging or shed turbulence. Thus, several investigators have established the validity of empirical formulations that relate radiated sound power to easily available aerodynamic and geometric parameters.

The most successful model of "in-pipe-generated spoiler noise" was developed by Gordon [Reference 27]; his model is based on the paramount assumption that there is a constant proportionality between the steady and fluctuating force components on a flow-spoiler. Under this assumption, the overall (and broadband) sound power, radiated from the end of a pipe due to an in-pipe located flow spoiler, can be related to the *steady-state* drag force acting on the spoiler.

The drag force on the spoiler is proportional to the product of the dynamic pressure on the spoiler, $1/2\rho U_c^2$ (where U_c is the "constricted velocity" as defined in Fig. 19), and the wake area of the spoiler. Under the assumption that flow is virtually potential down to the constriction point, and that atmospheric pressure penetrates up toward the spoiler location, the following relationship holds:

$$1/2\rho_1 U_1^2 + p_1 = 1/2\rho_a U_c^2 + p_a, \qquad (21)$$

where U_1 = upstream velocity

ρ_1 = upstream density

p_1 = upstream static pressure

U_c = constricted velocity

ρ_a = density at constriction point (approximately equal to outside density)

p_a = static pressure at constriction point, equal to outside pressure.

The left-hand side of Eq. 21 represents the total upstream pressure, p_t, so that Eq. 21 can be rewritten as

$$p_t - p_a = 1/2\rho_a U_c^2 , \qquad (22)$$

where $p_t - p_a$ is the total pressure drop across the spoiler.

The drag force F on the spoiler spanning the pipe diameter D then relates to the total pressure drop $\Delta p = p_t - p_a$, as

$$F \approx \Delta p \cdot (Dd), \qquad (23)$$

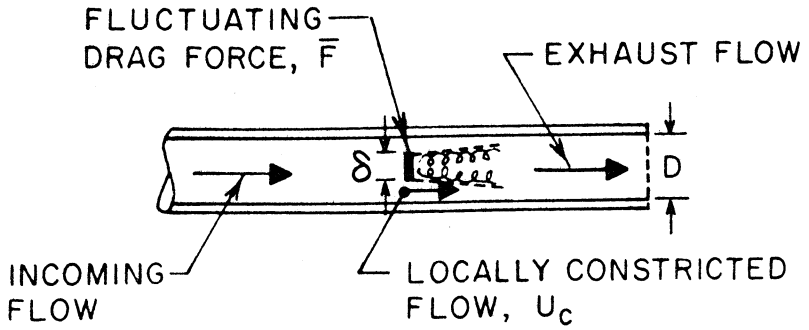

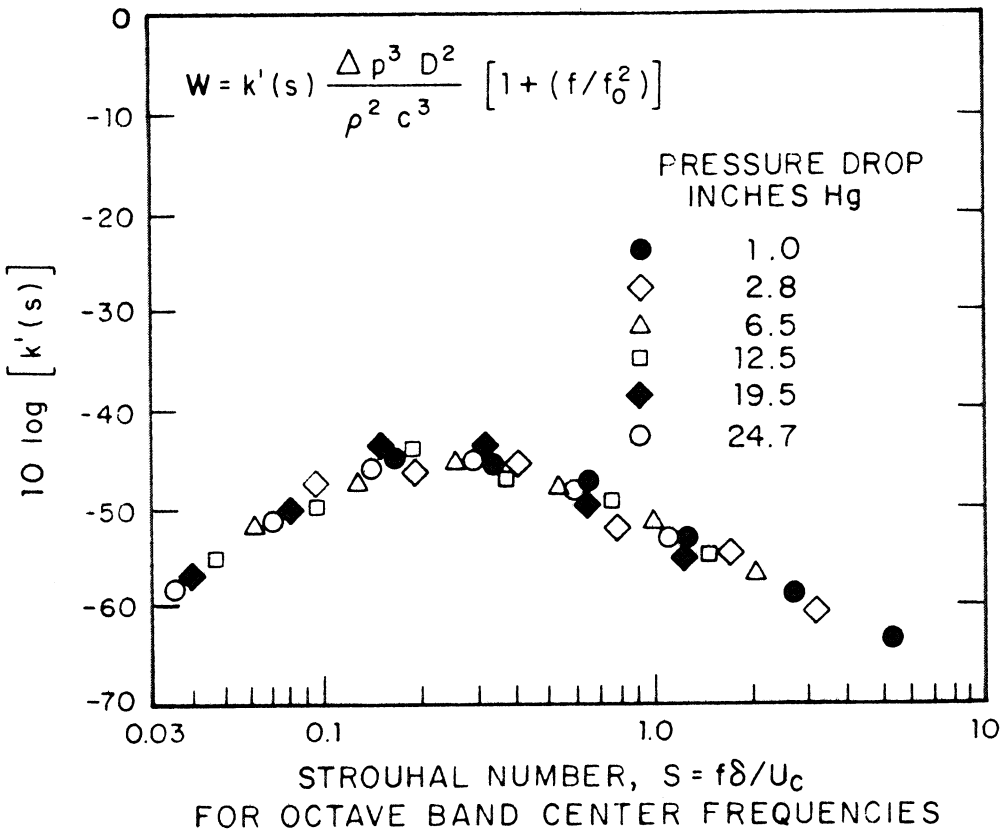

FIG. 19. EMPIRICAL CURVE FOR PREDICTION OF SPOILER NOISE

where (Dd) is the approximate wake area of the spoiler, D being the pipe diameter and d the spoiler width.

The dimensional relationship between acoustic power Π and (fluctuating) force amplitude F, frequency ω, atmospheric density ρ, and speed of sound c_0, was given previously by Eq. 19.

Again, the characteristic frequency of the aerodynamic forces is assumed to be proportional to the ratio of velocity and body dimension (U/d).

Thus,
$$\Pi \propto \rho^2 U_c^4 \left(\frac{U_c}{d}\right)^2 \cdot D^2 d^2 / \rho_a c_0^3 \qquad (24)$$

or

$$\Pi \propto \Delta p^3 \cdot D^2/\rho^2 c_0^3 \, . \qquad (25)$$

This formulation then relates sound power essentially to the pressure drop across the spoiler (rather than the force).

It is of particular interest that the spoiler geometry does not enter the formulation Eq. 25. This information is implicit in the pressure drop.

The constant of proportionality in Eq. 25

$$k \equiv \Pi/(\Delta p^3 D^2/\rho^2 c_0^3) \qquad (26)$$

was found to equal 2.5×10^{-4} for the overall broadband noise radiation for a wide variety of spoiler geometries.

Although the above formulation was found to be quite adequate to predict overall spoiler generated noise, it turned out to be less qualified as a basis for a "universal" non-dimensional spectrum for in-pipe generated spoiler noise. Normalization of measured spoiler spectra on the basis of Eq. 26, by plotting $k(s) = \Pi(s)/(\Delta p^3 D^2/\rho^2 c_0^3)$ vs Strouhal frequency $S = f\delta/U_c$, however, resulted in appreciable scatter at high Strouhal numbers, thus making the applicability of the dipole model over a large Mach number range questionable. However, by assuming the existence of aerodynamic quadrupole sources associated with spoiler-generated turbulence emanating into a quiescent space to dominate the radiation at high Strouhal numbers, a nondimensional power spectrum was found via the following procedures [References 14 and 23]:

At high Strouhal numbers, sound power from the pipe will be radiated according to

$$\Pi \propto \frac{\rho V^8 D^2}{c_0^5} \tag{27}$$

or, in terms of pressure drop across the spoiler,

$$\Pi \propto \frac{\Delta p^4 D^2}{\rho^3 c_0^5} \tag{28}$$

The crossover from one source mechanism to the other was found to occur at about the acoustic cut-off frequency of the pipe, f_0. Both mechanisms then appear under the new spectrum shape constant or k'(s)

$$k'(s) = \Pi \cdot \left[\left(\frac{\Delta p^3 D^2}{\rho^2 c_0^3} \right) \cdot \left(1 + \frac{f}{f_0}^2 \right) \right]^{-1}$$

The spectrum shape constant is plotted in logarithmic form vs Strouhal number in Fig. 19.

It is suggested to use this nondimensional spectrum for the prediction of in-pipe generated spoiler noise.

To determine the overall power level of sound radiated from the pipe exit due to an in-pipe located flow spoiler, Fig. 20 can be used, which is a parametric representation of Eq. 25. Sound power level in dB re 10^{-12} watt is related to total pressure drop Δp [in Newton/m] and pipe diameter [in cm].

The spectral peak occurs at a frequency given by

$$f_{peak} = 0.25\ U_c/d, \tag{29}$$

where d is the spoiler width and U_c is the constricted velocity, both in consistent units. U_c is given in Table I for several values of Δp:

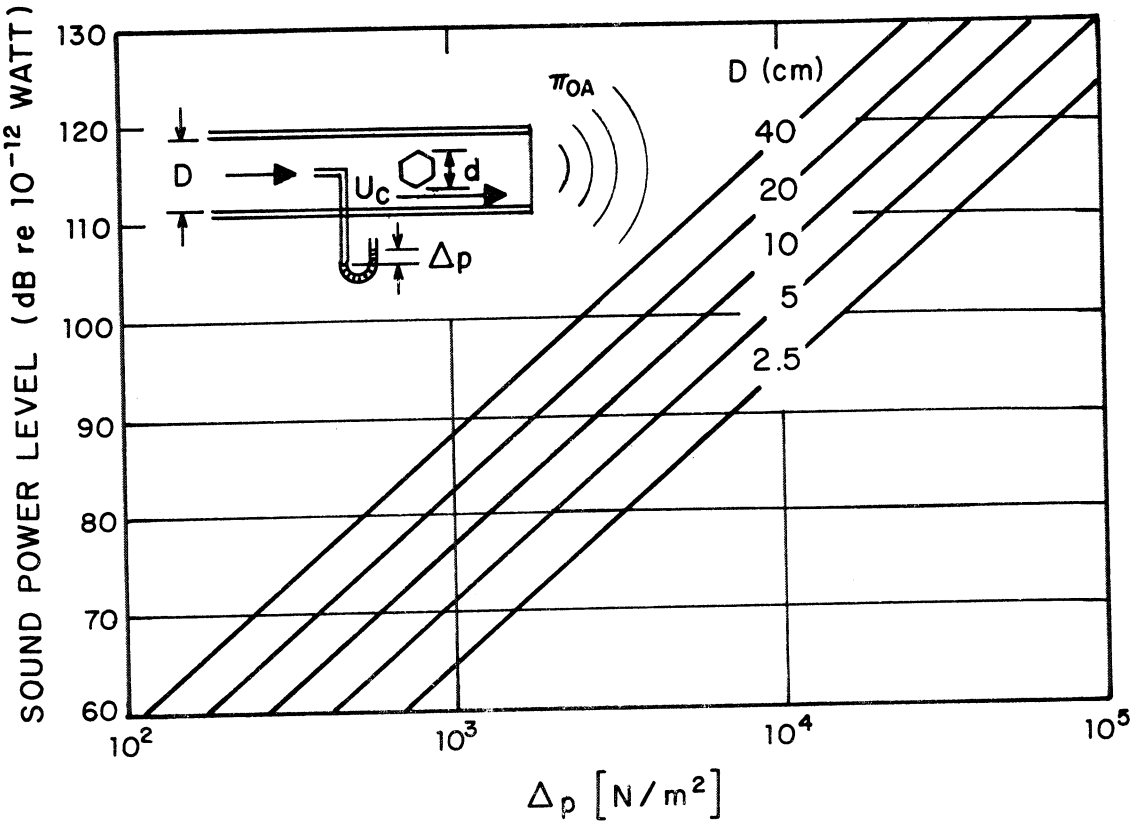

FIG. 20. NOMOGRAM FOR PREDICTING SPOILER NOISE FROM PRESSURE DROP AND DUCT DIAMETER

TABLE I

Δp (N/m^2)	2500	5000	10 000	20 000	40 000
U_c (m/sec)	63	90	124	173	238

The shape of the octave band spectrum is then given through Fig. 19, whereby the abscissa is directly proportional to frequency, since - for a particular case - both d and U_c are constant. The peak level of the spectrum is 8 dB below the overall level.

CLOSING

This report has treated some aspects of noise generation by the interaction of subsonic flow with rigid surfaces. Dipole-like sound fields were emphasized, although in practice one may observe additional sound which results from interaction of the fluid with itself ("quadrupole-like" sources) such as in the wake of a body or in the free shear layer of a wall jet type flow. Surface-generated noise ("direct radiation from the boundary layer") may also account for some additional observed sound.

This report has not treated all theories which pertain to the problem for reasons stated earlier - lack of experimental confirmation of theoretical predictions, lack of essential experimental inputs to semi-empirical models, and/or significant disagreement between observation and theoretical prediction.

In prediction of sound from flow interaction with surfaces, the current state-of-the-art reflects more a knowledge of gross trends than of exact prediction techniques. However, the knowledge accrued to date makes possible order of magnitude estimates of sound due to turbulent flow past trailing edges, sound arising from rigid surfaces operating in disturbed inflows, and sound from in-duct flow spoilers.

REFERENCES

1. Morse, P.M.; and Ingard, K.U.: Theoretical Acoustics. McGraw-Hill, 1968.

2. Ribner, H.S.: The Generation of Sound by Turbulent Jets. Advances Appl. Mech., Vol. 8, 1964.

3. Hayden, R.E.: Sound Generation by Turbulent Wall Jet Flow over a Trailing Edge. M.S. Thesis, Purdue Univ., 1969.

4. Hayden, R.E.; and Chanaud, R.C.: Sound Generation by Turbulent Wall Jet Flow over a Trailing Edge. Paper FF-10, Spring Meeting of the Acoust. Soc. Am. (Atlantic City, N.J.), 1970.

5. Chanaud, R.C.; and Hayden, R.E.: Edge Sound Produced by Two Turbulent Wall Jets. Paper FF-11, Spring Meeting of the Acoust. Soc. Am. (Atlantic City, N.J.), 1970.

6. Curle, N.: The Influence of Solid Boundaries upon Aerodynamic Sound, Proc. Roy. Soc. (London), A231, 1955.

7. Grosche, F.R.: On the Generation of Sound Resulting From the Passage of a Turbulent Air Jet Over a Flat Plate of Finite Dimensions., R.A.E. Library Translation No. 1460, Oct. 1970.

8. Yildiz, M.; and Mawardi, O.K.: On the Diffraction of Multipole Fields by a Semi-Infinite Wedge. J. Acoust. Soc. Am., Vol. 32, No. 12, 1960.

9. Bender, E.K.; Hayden, R.E.; and Heller, H.H.: Analysis of Potential Noise Sources of the Tracked Air Cushion Vehicle. BBN Rept. 2178; also, DOT-TSC-194-1, July 1971.

10. Hersh, A.S.; and Hayden, R.E.: Aerodynamic Noise from Airfoils with and without Leading Edge Serrations. BBN Rept. 2095, June 1971.

11. Unfried, H.: M.S. Thesis, Univ. of Calif. (Los Angeles), 1960.

12. Powell A.: On the Edgetone. J. Acoust. Soc. Am., Vol. 33 (1), No. 4, 1961.

13. Sharland, I.J.: Sources of Noise in Axial Flow Fans. J. Sound Vib., Vol. 1, No. 3, 1964.

REFERENCES (Cont.)

14. Heller, H.H.; and Widnall. S.: Correlation of Fluctuating Forces with the Sound Radiated from Rigid Flow Spoilers. BBN Report 1734, 1968; also, J. Acoust. Soc. Am., Vol. 47 (2), No. 3, 1970.

15. Clark, P.J.F.; and Ribner, H.S.: Direct Correlation of Fluctuating Lift and Radiated Sound for an Airfoil in Turbulent Flow. J. Acoust. Soc. Am., Vol. 46 (2), No. 3, 1969.

16. Von Karman, T.; and Sears, W.R.: Airfoil Theory for Non-Uniform Motion. J. Aero. Sci., Vol. 5, No. 10, Aug. 1938.

17. Sears, W.R.: Some Aspects of Non-Stationary Airfoil Theory and Its Practical Application. J. Aero. Sci., Vol. 8, No. 3, Jan. 1941.

18. Leipmann, H.W.: On the Application of Statistical Concepts to the Buffeting Problem. J. Aero. Sci., Vol. 19, 1952.

19. Bisplinghoff, R.L.; Ashley, H.; and Halfman, R.L.: Aeroelasticity. Addison-Wesley Publishing Co., Inc., 1955.

20. Filotas, L.T.: Theory of Airfoil Response in a Gusty Atmosphere; Part II - Response to Discrete Gusts of Continuous Turbulence. UTIAS Rept. 141, Nov. 1969.

21. Theodorsen, T.: General Theory of Aerodynamic Instability and the Mechanism of Flutter. NACA Rept. 436, 1935.

22. Hayden, R.E.: Noise Generation by Duct Elements in Low Speed Airflows. Presented at Purdue Univ. Conf. on Noise Control, July 14-16, 1971.; also, BBN Rept. 2009, 1970.

23. Bender, E.K.: Hydrofoil Design for Minimum Control Power. Ongoing study (Contract N00014-70-C-0032, Naval Ship Research and Development Center), Bolt Beranek and Newman Inc.

24. Mugridge, B.D.: Sound Radiation from Airfoils in Turbulent Flow. J. Sound Vib., Vol. 13, Nov. 1970.

REFERENCES (Cont.)

25. Mugridge, B.D.: The Generation and Radiation of Acoustic Energy by the Blades of a Subsonic Axial Flow Fan Due to Unsteady Flow Interaction. Ph.D. Thesis, U. of Southampton, 1970.

26. Dean, L.W.: Broadband Noise Generation by Airfoils in Turbulent Flow. AIAA Paper 71-587 (Palo Alto, Calif.), June 1971.

27. Gordon, C.G.: Spoiler-Generated Flow Noise. BBN Rept. 1426 (with G. Maidanik); also, NASA CR-69-679, 1967; also, J. Acoust. Soc. Am., Vol. 45, No. 1, 1969.

NASA-Langley, 1972 —— 2 CR-2126